Eur. Phys. J. B (2013) 86: 115
DOI: 10.1140/epjb/e2013-31157-6

THE EUROPEAN PHYSICAL JOURNAL B

Regular Article

On the theory of superconductivity in the extended Hubbard model

Spin-fluctuation pairing

Nikolay M. Plakida[1,2,a] and Viktor S. Oudovenko[3]

[1] Joint Institute for Nuclear Research, 141980 Dubna, Russia
[2] Max-Planck-Institut für Physik komplexer Systeme, 01187 Dresden, Germany
[3] Rutgers University, 08854 New Jersey, USA

Received 27 December 2012 / Received in final form 17 January 2013
Published online 25 March 2013 –

Abstract. A microscopic theory of superconductivity in the extended Hubbard model which takes into account the intersite Coulomb repulsion and electron-phonon interaction is developed in the limit of strong correlations. The Dyson equation for normal and pair Green functions expressed in terms of the Hubbard operators is derived. The self-energy is obtained in the noncrossing approximation. In the normal state, antiferromagnetic short-range correlations result in the electronic spectrum with a narrow bandwidth. We calculate superconducting T_c by taking into account the pairing mediated by charge and spin fluctuations and phonons. We found the d-wave pairing with high-T_c mediated by spin fluctuations induced by the strong kinematic interaction for the Hubbard operators. Contributions to the d-wave pairing coming from the intersite Coulomb repulsion and phonons turned out to be small.

1 Introduction

Despite intensive studies of high-temperature superconductivity (HTSC) in cuprates for many years after the discovery of Bednorz and Müller [1], a commonly accepted mechanism of HTSC is still lacking (see, e.g. [2,3]). A good candidate from various proposed mechanisms is based on a model of strongly correlated electrons [4,5]. In the model, superconductivity occurs at finite doping in the resonating valence bond state (RVB) due to the antiferromagnetic (AF) superexchange in the t-J model. A possibility of HTSC mediated by AF spin fluctuations as a "glue" for superconducting pairing was also considered [6], mostly within phenomenological spin-fermion models (see, e.g., [7–12], and references therein).

Recent studies of spin-excitations by magnetic inelastic neutron scattering (INS) and the electronic spectrum by angle-resolved photoemission spectroscopy (ARPES) have revealed an important role of AF spin excitations in the "kink" phenomenon and the d-wave pairing in cuprates (see, e.g., [13] and references therein). In particular, in reference [14] using INS and ARPES studies on the same $YBa_2Cu_3O_{6.6}$ ($YBCO_{6.6}$) crystal, an estimation for superconducting $T_c \sim 150$ K was found. The main argument against the spin-fluctuation pairing, the weak intensity of spin fluctuations at the optimal doping seen in INS experiments [15], was dismissed in the recent resonant inelastic X-ray scattering experiments [16]. In a large family of cuprate superconductors, paramagnon AF excitations with the dispersion and spectral weight similar to those of magnons in undoped cuprates were observed. Using the magnetic spectrum found in the $YBCO_7$ crystal, superconductivity with $T_c = 100{-}200$ K was predicted. Thus, spin fluctuations have sufficient strength to mediate HTSC in cuprates and to explain various physical properties of cuprate materials as, e.g., the optical conductivity [17]. Therefore, it can be suggested that the alternative mechanism based on the conventional electron-phonon interaction (EPI) (see, e.g., [18,19]) plays a secondary role in the cuprate superconductors.

Recently, in reference [20] using the renormalization group (RG) method, an asymptotically exact solution for the d-wave pairing was found in the conventional Hubbard model [21] in the weak correlation limit, $U \ll t$. However, as was pointed out later in reference [22], a contribution from the repulsive well-screened weak Coulomb interaction (CI) in the first order strongly suppresses the pairing induced by the contributions of higher orders, and a possibility for superconductivity "from repulsion" was questioned. At the same time, in reference [23] it was shown that the p-wave superconductivity exists in the electronic gas at low density with a strong repulsion U and a relatively strong Coulomb intersite interaction V_{ij} (see, also [24] and references therein). Later on, in reference [25] RG studies of the extended Hubbard model with the intersite interaction have shown that superconducting pairing

[a] e-mail: plakida@theor.jinr.ru

of various symmetries, extended s-, p-, and d-wave types, can occur depending on the electron concentration and the intersite interaction V_{ij}. However, in these investigations the Fermi-liquid model in the weak correlation limit was used. To study superconductivity in cuprates, the Mott-Hubbard (more accurately, charge-transfer) doped insulators, a theory of strongly correlated electronic systems should be used (for reviews see [26,27]).

In the present paper we consider superconductivity in the extended Hubbard model with a weak intersite Coulomb repulsion V_{ij} but in comparison with references [20,22,25], we study the limit of strong correlations, $U \gg t$. To compare various contributions to the superconducting d-wave pairing, we consider also a model of the EPI with strong forward scattering proposed in reference [28]. The Dyson equation for the thermodynamic Green functions (GFs) expressed in terms of the Hubbard operators (HOs) is derived using the Mori-type projection technique [29]. The self-energy is calculated in the noncrossing approximation (NCA) as in the microscopic theory of the electronic spectrum in the normal state in our previous publication [30]. We show that the kinematic interaction for the HOs generates the AF superexchange pairing similar to the t-J model. A contribution from the intersite Coulomb repulsion in the first order suppresses the pairing as found in references [22,25]. But the kinematic interaction induces also a strong electron interaction with spin-fluctuations which results in the d-wave superconductivity with high-T_c. Contribution from the EPI to the d-wave pairing turned out to be small.

In the next section we introduce the model, derive the Dyson equation, and calculate the self-energy in the NCA. A self-consistent system of equations is formulated in Section 3. Results of computations of the electronic spectrum in the normal state and of superconducting T_c and the d-wave gap function are presented in Section 4. Concluding remarks are given in Section 5.

2 General formulation

2.1 Extended Hubbard model

We consider an extended Hubbard model on a square lattice which we write in terms of the HOs [31]:

$$H = \varepsilon_1 \sum_{i,\sigma} X_i^{\sigma\sigma} + \varepsilon_2 \sum_i X_i^{22} + \sum_{i\neq j,\sigma} \{ t_{ij}^{11} X_i^{\sigma 0} X_j^{0\sigma} + t_{ij}^{22} X_i^{2\sigma} X_j^{\sigma 2} + \sigma t_{ij}^{12} (X_i^{2\bar{\sigma}} X_j^{0\sigma} + \text{H.c.}) \} + H_{c,ep}. \quad (1)$$

To apply the model for consideration of the cuprate superconductors, we introduce the HOs for holes taking into account four possible states on a lattice site i: an empty state $(\alpha, \beta = 0)$, a singly occupied hole state $(\alpha, \beta = \sigma)$ with the spin $\sigma/2 = \pm(1/2)$, $\bar{\sigma} = -\sigma$, and a two-hole state $(\alpha, \beta = 2)$. Then the HO $X_i^{\alpha\beta} = |i\alpha\rangle\langle i\beta|$ describes the transition from the state $|i, \beta\rangle$ to the state $|i, \alpha\rangle$. Energy parameters in the model (1) are taken close to the values found within the cell-perturbation method [32] for the p-d model for the CuO_2 plane [33,34]. In particular, the single-particle energy $\varepsilon_1 = \varepsilon_d - \mu$ is the energy of the d-type one-hole state measured from the chemical potential μ and the two-particle energy $\varepsilon_2 = 2\varepsilon_1 + U$ is the energy of the two-hole p-d Zhang-Rice singlet state [35]. The effective Hubbard U in cuprates is the charge-transfer energy $U = \Delta_{pd} = \epsilon_p - \epsilon_d$. According to the cell perturbation method, in general case the values of the hopping parameters $t_{ij}^{\eta\zeta}$ in (1) depends on the subband indices η, $\zeta = 1, 2$.

In the last term in (1) in addition to the intersite CI V_{ij} for holes in the plane we take into account also the EPI g_{ij} for holes with phonons:

$$H_{c,ep} = \frac{1}{2} \sum_{i\neq j} V_{ij} N_i N_j + \sum_{i,j} g_{ij} N_i u_j, \quad (2)$$

where u_j describes an atomic displacement on the lattice site j for a particular phonon mode. More generally, the EPI can be written as a sum $\sum_\nu g_{i,j}^\nu u_j^\nu$ over the normal modes ν. The hole number operator and the spin operators in terms of HOs are defined as

$$N_i = \sum_\sigma X_i^{\sigma\sigma} + 2X_i^{22}, \quad (3)$$

$$S_i^\sigma = X_i^{\sigma\bar{\sigma}}, \quad S_i^z = (\sigma/2)\,[X_i^{\sigma\sigma} - X_i^{\bar{\sigma}\bar{\sigma}}]. \quad (4)$$

The completeness relation for the HOs, $X_i^{00} + \sum_\sigma X_i^{\sigma\sigma} + X_i^{22} = 1$, rigorously preserves the constraint of no double occupancy of the quantum state α on any lattice site i. From the multiplication rule $X_i^{\alpha\beta} X_i^{\gamma\delta} = \delta_{\beta\gamma} X_i^{\alpha\delta}$ follows the commutation relations:

$$\left[X_i^{\alpha\beta}, X_j^{\gamma\delta} \right]_\pm = \delta_{ij} \left(\delta_{\beta\gamma} X_i^{\alpha\delta} \pm \delta_{\delta\alpha} X_i^{\gamma\beta} \right). \quad (5)$$

The upper sign refers to the Fermi-type operators like $X_i^{0\sigma}$ while the lower sign refers to the Bose-type operators like N_i (3) or the spin operators (4).

The chemical potential μ depends on the average *hole* occupation number

$$n = 1 + \delta = \langle N_i \rangle, \quad (6)$$

where $\langle ... \rangle$ denotes the statistical average with the Hamiltonian (1).

We emphasize here that the Hubbard model (1) does not involve a dynamical coupling of electrons (holes) to fluctuations of spins or charges. Its role is played by the *kinematic* interaction caused by the complicated commutation relations (5), as was already noted by Hubbard [31]. For example, the equation of motion for the HO $X_i^{\sigma 2}$ in

the Heisenberg representation ($\hbar = 1$) reads,

$$i\frac{d}{dt}X_i^{\sigma 2} = [X_i^{\sigma 2}, H] = (\varepsilon_1 + U)\, X_i^{\sigma 2} + \sum_{l,\sigma'}\left(t_{il}^{22} B_{i\sigma\sigma'}^{22} X_l^{\sigma' 2} - \sigma t_{il}^{21} B_{i\sigma\sigma'}^{21} X_l^{0\bar{\sigma}'}\right) - \sum_l X_i^{02}\left(t_{il}^{11} X_l^{\sigma 0} + \sigma t_{il}^{21} X_l^{2\bar{\sigma}}\right) + \sum_l X_i^{\sigma 2}(V_{il}\, N_l + g_{il}\, u_l). \quad (7)$$

Here $B_{i\sigma\sigma'}^{\eta\zeta}$ are the Bose-like operators,

$$B_{i\sigma\sigma'}^{22} = (X_i^{22} + X_i^{\sigma\sigma})\,\delta_{\sigma'\sigma} + X_i^{\sigma\bar{\sigma}}\,\delta_{\sigma'\bar{\sigma}} = (N_i/2 + \sigma\, S_i^z)\,\delta_{\sigma'\sigma} + S_i^{\sigma}\,\delta_{\sigma'\bar{\sigma}}, \quad (8)$$

$$B_{i\sigma\sigma'}^{21} = (N_i/2 + \sigma S_i^z)\,\delta_{\sigma'\sigma} - S_i^{\sigma}\,\delta_{\sigma'\bar{\sigma}}, \quad (9)$$

where we used the definition of the number operator (3) and the spin operators (4). The last term in (7) is caused by the dynamic intersite CI and the EPI.

2.2 Dyson equation

To consider the superconducting pairing in the model (1), we introduce the two-time thermodynamic GF [36,37] expressed in terms of the four-component Nambu operators, $\hat{X}_{i\sigma}$ and $\hat{X}_{i\sigma}^{\dagger} = (X_i^{2\sigma}\ X_i^{\bar{\sigma}0}\ X_i^{\bar{\sigma}2}\ X_i^{0\sigma})$:

$$\mathsf{G}_{ij\sigma}(t-t') = -i\theta(t-t')\langle\{\hat{X}_{i\sigma}(t), \hat{X}_{j\sigma}^{\dagger}(t')\}\rangle \equiv \langle\langle \hat{X}_{i\sigma}(t) \mid \hat{X}_{j\sigma}^{\dagger}(t')\rangle\rangle, \quad (10)$$

where $\{A, B\} = AB + BA$, $A(t) = \exp(iHt)A\exp(-iHt)$, and $\theta(x) = 1$ for $x > 0$ and $\theta(x) = 0$ for $x < 0$. The Fourier representation in $(\mathbf{k}, \omega)$-space is defined by the relations:

$$\mathsf{G}_{ij\sigma}(t-t') = \frac{1}{2\pi}\int_{-\infty}^{\infty} dt e^{-i(t-t')}\mathsf{G}_{ij\sigma}(\omega), \quad (11)$$

$$\mathsf{G}_{ij\sigma}(\omega) = \frac{1}{N}\sum_{\mathbf{k}}\exp[i\mathbf{k}(\mathbf{i}-\mathbf{j})]\mathsf{G}_{\sigma}(\mathbf{k},\omega). \quad (12)$$

The GF (11) is convenient to write in the matrix form

$$\mathsf{G}_{ij\sigma}(\omega) = \begin{pmatrix} \hat{G}_{ij\sigma}(\omega) & \hat{F}_{ij\sigma}(\omega) \\ \hat{F}_{ij\sigma}^{\dagger}(\omega) & -\hat{G}_{ji\bar{\sigma}}(-\omega)\end{pmatrix}, \quad (13)$$

where the normal $\hat{G}_{ij\sigma}$ and anomalous (pair) $\hat{F}_{ij\sigma}$ GFs are the 2×2 matrices for two Hubbard subbands:

$$\hat{G}_{ij}(\omega) = \left\langle\left\langle \begin{pmatrix} X_i^{\sigma 2} \\ X_i^{0\bar{\sigma}}\end{pmatrix} \middle| X_j^{2\sigma} X_j^{\bar{\sigma}0}\right\rangle\right\rangle_{\omega}, \quad (14)$$

$$\hat{F}_{ij}(\omega) = \left\langle\left\langle \begin{pmatrix} X_i^{\sigma 2} \\ X_i^{0\bar{\sigma}}\end{pmatrix} \middle| X_j^{\bar{\sigma}2} X_j^{0\sigma}\right\rangle\right\rangle_{\omega}. \quad (15)$$

To calculate the GF (10) we use the equation of motion method. Differentiating the GF with respect to time t, the Fourier representation of it leads to the equation

$$\omega\mathsf{G}_{ij\sigma}(\omega) = \delta_{ij}\mathsf{Q} + \langle\langle[\hat{X}_{i\sigma}, H] \mid \hat{X}_{j\sigma}^{\dagger}\rangle\rangle_{\omega}. \quad (16)$$

Here the correlation function $\mathsf{Q} = \langle\{\hat{X}_{i\sigma}, \hat{X}_{i\sigma}^{\dagger}\}\rangle = \hat{\tau}_0 \times \hat{Q}$ where $\hat{Q} = \begin{pmatrix} Q_2 & 0 \\ 0 & Q_1\end{pmatrix}$ and $\hat{\tau}_0$ is the 2×2 unit matrix. The spectral weights of the Hubbard subbands in the paramagnetic state $Q_2 = \langle X_i^{22} + X_i^{\sigma\sigma}\rangle = n/2$ and $Q_1 = \langle X_i^{00} + X_i^{\bar{\sigma}\bar{\sigma}}\rangle = 1 - Q_2$ depend on the occupation number of holes (6). In the Q matrix we neglect anomalous averages of the type $\langle X_i^{02}\rangle$ which are irrelevant for the d-wave pairing [38].

To introduce the zero-order quasiparticle (QP) excitation energy we use the Mori-type projection method [29]. In this approach, the many-particle operator $\hat{Z}_{i\sigma} = [\hat{X}_{i\sigma}, H]$ in (16) is written as a sum of a linear part and an irreducible part $\hat{Z}_{i\sigma}^{(ir)}$ orthogonal to $\hat{X}_{j\sigma}^{\dagger}$:

$$\hat{Z}_{i\sigma} = [\hat{X}_{i\sigma}, H] = \sum_l \mathsf{E}_{il\sigma}\hat{X}_{l\sigma} + \hat{Z}_{i\sigma}^{(\mathrm{ir})}. \quad (17)$$

The orthogonality condition $\langle\{\hat{Z}_{i\sigma}^{(\mathrm{ir})}, \hat{X}_{j\sigma}^{\dagger}\}\rangle = 0$ determines the excitation energy in the mean-field approximation (MFA)

$$\mathsf{E}_{ij\sigma} = \langle\{[\hat{X}_{i\sigma}, H], \hat{X}_{j\sigma}^{\dagger}\}\rangle\mathsf{Q}^{-1} = (1/N)\sum_{\mathbf{k}}\exp[i\mathbf{k}(\mathbf{i}-\mathbf{j})]\,\mathsf{E}_{\sigma}(\mathbf{k}), \quad (18)$$

and the corresponding zero-order GF

$$\mathsf{G}_{\sigma}^{0}(\mathbf{k},\omega) = \left(\omega\tilde{\tau}_0 - \mathsf{E}_{\sigma}(\mathbf{k})\right)^{-1}\mathsf{Q}, \quad (19)$$

where $\tilde{\tau}_0$ is the 4×4 unit matrix.

To calculate the multiparticle GF $\langle\langle\hat{Z}_{i\sigma}^{(\mathrm{ir})}(t) \mid \hat{X}_{j\sigma}^{\dagger}(t')\rangle\rangle$ in (16) we differentiate it with respect to the second time t' and apply the same projection procedure as in (17). This results in the equation for the GF (16) in the form,

$$\mathsf{G}_{\sigma}(\mathbf{k},\omega) = \mathsf{G}_{\sigma}^{0}(\mathbf{k},\omega) + \mathsf{G}_{\sigma}^{0}(\mathbf{k},\omega)\,\mathsf{T}_{\sigma}(\mathbf{k},\omega)\,\mathsf{G}_{\sigma}^{0}(\mathbf{k},\omega), \quad (20)$$

where the scattering matrix

$$\mathsf{T}_{\sigma}(\mathbf{k},\omega) = \mathsf{Q}^{-1}\,\langle\langle\hat{Z}_{\mathbf{k}\sigma}^{(\mathrm{ir})} \mid \hat{Z}_{\mathbf{k}\sigma}^{(\mathrm{ir})\dagger}\rangle\rangle_{\omega}\,\mathsf{Q}^{-1}. \quad (21)$$

Now we can introduce the self-energy operator $\Sigma_{\sigma}(\mathbf{q},\omega)$ as the *proper* part (pp) of the scattering matrix (21) which has no parts connected by the zero-order GF (19) according to the equation: $\mathsf{T} = \Sigma + \Sigma\,\mathsf{G}^0\,\mathsf{T}$. The definition of the proper part of the scattering matrix (21) is equivalent to an introduction of a projected Liouvillian superoperator for the memory function in the conventional Mori technique [29].

Using the self-energy operator instead of the scattering matrix in equation (20) we obtain the Dyson equation for the GF (10):

$$\mathsf{G}_{\sigma}(\mathbf{k},\omega) = [\omega\tilde{\tau}_0 - \mathsf{E}_{\sigma}(\mathbf{k}) - \mathsf{Q}\Sigma_{\sigma}(\mathbf{k},\omega)]^{-1}\,\mathsf{Q}, \quad (22)$$

where the self-energy operator is given by

$$\mathsf{Q}\Sigma_\sigma(\mathbf{k},\omega) = \langle\langle \hat{Z}^{(\mathrm{ir})}_{\mathbf{k}\sigma} \,|\, \hat{Z}^{(\mathrm{ir})\dagger}_{\mathbf{k}\sigma} \rangle\rangle^{(\mathrm{pp})}_{\omega}\, \mathsf{Q}^{-1}. \tag{23}$$

Dyson equation (22) with the zero-order QP excitation energy (18) and the self-energy (23) gives an exact representation for the GF (10). The self-energy takes into account processes of inelastic scattering of electrons (holes) on spin and charge fluctuations due to the kinematic interaction and the dynamic intersite CI and the EPI (see Eq. (7)). To obtain a closed system of equations, the multiparticle GF in the self-energy operator (23) should be evaluated as discussed below.

3 Self-consistent system of equations

3.1 Mean-field approximation

The superconducting pairing in the Hubbard model already occurs in the MFA and is caused by the kinetic superexchange interaction as in the t-J model [4,5]. Therefore, it is reasonable to consider at first the MFA described by the zero-order GF (19). Using commutation relations (5) for the HOs we calculate the energy matrix (18):

$$\mathsf{E}_{ij\sigma} = \begin{pmatrix} \hat{\varepsilon}_{ij} & \hat{\Delta}_{ij\sigma} \\ \hat{\Delta}^*_{ji\sigma} & -\hat{\varepsilon}_{ji\bar{\sigma}} \end{pmatrix}. \tag{24}$$

The matrix $\hat{\varepsilon}(\mathbf{k}) = \sum_j \exp[i\mathbf{k}(\mathbf{i}-\mathbf{j})]\hat{\varepsilon}_{ij}$ after diagonalization determines the QP spectrum in the two Hubbard subbands in the normal state (for details see [30]):

$$\varepsilon_{1,2}(\mathbf{k}) = (1/2)[\omega_2(\mathbf{k}) + \omega_1(\mathbf{k})] \mp (1/2)\Lambda(\mathbf{k}), \tag{25}$$

$$\omega_\iota(\mathbf{k}) = 4t\,\alpha_\iota\gamma(\mathbf{k}) + 4\,\beta_\iota\, t'\gamma'(\mathbf{k}) + 4\,\beta_\iota\, t''\gamma''(\mathbf{k}) + \omega^{(c)}_\iota(\mathbf{k}) + U\delta_{\iota,2} - \mu, \quad (\iota = 1,2) \tag{26}$$

$$\Lambda(\mathbf{k}) = \{[\omega_2(\mathbf{k}) - \omega_1(\mathbf{k})]^2 + 4W(\mathbf{k})^2\}^{1/2},$$

$$W(\mathbf{k}) = 4t\,\alpha_{12}\gamma(\mathbf{k}) + 4t'\,\beta_{12}\gamma'(\mathbf{k}) + 4t''\,\beta_{12}\gamma''(\mathbf{k}).$$

Here the hopping parameters in (1) are assumed to be equal, $t^{22}_{ij} = t^{11}_{ij} = t^{12}_{ij} = t_{ij}$, where t_{ij} is defined by the expression:

$$t_{ij} = (1/N)\sum_{\mathbf{k}} \exp[i\mathbf{k}(\mathbf{i}-\mathbf{j})]\, t(\mathbf{k}), \tag{27}$$

$$t(\mathbf{k}) = 4t\,\gamma(\mathbf{k}) + 4t'\,\gamma'(\mathbf{k}) + 4t''\,\gamma''(\mathbf{k}). \tag{28}$$

The hopping parameters are equal to t for the nearest neighbor (n.n.) sites $a_1 = (\pm a_x, \pm a_y)$, t' – for the next nearest neighbor (n.n.n.) sites $a_d = \pm(a_x \pm a_y)$, and t'' – for the n.n.n. sites $a_2 = \pm 2a_x, \pm 2a_y$. The corresponding $\mathbf{k}$-dependent functions are: $\gamma(\mathbf{k}) = (1/2)(\cos k_x + \cos k_y)$, $\gamma'(\mathbf{k}) = \cos k_x \cos k_y$, and $\gamma''(\mathbf{k}) = (1/2)(\cos 2k_x + \cos 2k_y)$ (the lattice constants $a_x = a_y$ are put to unity). The contribution from the CI V_{ij} in (26) is given by

$$\omega^{(c)}_{1(2)}(\mathbf{k}) = \frac{1}{N}\sum_{\mathbf{q}} V(\mathbf{k}-\mathbf{q}) N_{1(2)}(\mathbf{q}), \tag{29}$$

where $N_1(\mathbf{q}) = \langle X^{0\bar{\sigma}}_{\mathbf{q}} X^{\bar{\sigma}0}_{\mathbf{q}}\rangle/Q_1$, $N_2(\mathbf{q}) = \langle X^{\sigma 2}_{\mathbf{q}} X^{2\sigma}_{\mathbf{q}}\rangle/Q_2$ and $V(\mathbf{k}-\mathbf{q})$ is the Fourier transform of V_{ij}.

The kinematic interaction for the HOs results in renormalization of the spectrum (25) determined by the parameters: $\alpha_\iota = Q_\iota[1 + C_1/Q^2_\iota]$, $\beta_\iota = Q_\iota[1 + C_2/Q^2_\iota]$, $\alpha_{12} = \sqrt{Q_1Q_2}[1 - C_1/Q_1Q_2]$, $\beta_{12} = \sqrt{Q_1Q_2}[1 - C_2/Q_1Q_2]$. Here we take into account the renormalization caused by the spin correlation functions for the n.n. and the n.n.n. sites, respectively:

$$C_1 = \langle \mathbf{S}_i\mathbf{S}_{i+a_1}\rangle, \quad C_2 = \langle \mathbf{S}_i\mathbf{S}_{i+a_d}\rangle \approx \langle \mathbf{S}_i\mathbf{S}_{i+a_2}\rangle. \tag{30}$$

The short-range AF correlations considerably suppress the n.n. hopping parameters since $C_1 < 0$ and at low doping $|C_1| = 0.1$–0.2 that results in $\alpha_\iota \ll 1$. At the same time, the n.n.n. hopping parameters are increased since $C_2 > 0$.

Now we evaluate the anomalous components $\hat{\Delta}_{ij\sigma}$ of the matrix (24) which determine the superconducting gap in the MFA. Considering the singlet d-wave pairing, we calculate the intersite pair correlation functions. The diagonal matrix components are given by the equations:

$$\Delta^{22}_{ij\sigma} Q_2 = -\sigma\, t^{21}_{ij}\langle X^{02}_i N_j\rangle - V_{ij}\langle X^{\sigma 2}_i\, X^{\bar{\sigma}2}_j\rangle, \tag{31}$$

$$\Delta^{11}_{ij\sigma} Q_1 = \sigma\, t^{12}_{ij}\langle N_j X^{02}_i\rangle - V_{ij}\langle X^{0\bar{\sigma}}_i X^{0\sigma}_j\rangle. \tag{32}$$

Here we used the original notation for the interband hopping parameters t^{12}_{ij} to emphasize that the kinematic pairing $\langle X^{02}_i N_j\rangle$ is mediated by the interband hopping. In terms of the Fermi operators $a_{i\sigma} = X^{0\sigma}_i + \sigma X^{\bar{\sigma}2}_i$, the pair correlation function in (31) can be written as $\langle X^{02}_i N_j\rangle = \langle X^{0\downarrow}_i X^{\downarrow 2}_i N_j\rangle = \langle a_{i\downarrow}\, a_{i\uparrow} N_j\rangle$. This representation shows that the kinematic pairing occurs on a single lattice site but in two Hubbard subbands [39].

The correlation function $\langle X^{02}_i N_j\rangle$ can be calculated directly from the GF $L_{ij}(t-t') = \langle\langle X^{02}_i(t) | N_j(t')\rangle\rangle$ without *any decoupling* approximation as shown in reference [39]. In particular, under hole doping, $n = 1 + \delta > 1$, the pair correlation function in the two-site approximation reads:

$$\langle X^{02}_i N_j\rangle = -\frac{4t^{12}_{ij}}{U}\sigma\,\langle X^{\sigma 2}_i X^{\bar{\sigma}2}_j\rangle. \tag{33}$$

As a result, the equation for the superconducting gap in (31) can be written as

$$\Delta^{22}_{ij\sigma} = (J_{ij} - V_{ij})\,\langle X^{\sigma 2}_i X^{\bar{\sigma}2}_j\rangle/Q_2, \tag{34}$$

where $J_{ij} = 4\,(t^{12}_{ij})^2/U$ is the AF superexchange interaction. A similar equation holds for the gap in the one-hole subband: $\Delta^{11}_{ij\sigma} = (J_{ij} - V_{ij})\,\langle X^{0\bar{\sigma}}_i X^{0\sigma}_j\rangle/Q_1$. We thus conclude that the pairing in the Hubbard model in the MFA is similar to the superconductivity in the t-J model mediated by the AF superexchange interaction J_{ij}.

3.2 Self-energy operator

Self-energy operator (23) can be written in the same matrix form as the GF (13):

$$\mathsf{Q}\,\Sigma_{ij\sigma}(\omega) = \begin{pmatrix} \hat{M}_{ij\sigma}(\omega) & \hat{\Phi}_{ij\sigma}(\omega) \\ \hat{\Phi}^\dagger_{ij\sigma}(\omega) & -\hat{M}_{ji\bar{\sigma}}(-\omega) \end{pmatrix}\mathsf{Q}^{-1}, \tag{35}$$

where the matrices $\hat{M}$ and $\hat{\Phi}$ denote the respective normal and anomalous (pair) components of the self-energy operator. The system of equations for the (4×4) matrix GF (13) and the self-energy (35) can be reduced to a system of equations for the normal $\hat{G}_\sigma(\mathbf{k},\omega)$ and the pair $\hat{F}_\sigma(\mathbf{k},\omega)$ (2×2) matrix components. Using representations for the energy matrix (24) and the self-energy (35), we derive for these components the following system of matrix equations:

$$\hat{G}(\mathbf{k},\omega) = \Big(\hat{G}_N(\mathbf{k},\omega)^{-1} + \hat{\varphi}_\sigma(\mathbf{k},\omega)\,\hat{G}_N(\mathbf{k},-\omega)\,\hat{\varphi}^*_\sigma(\mathbf{k},\omega)\Big)^{-1}\hat{Q}, \quad (36)$$

$$\hat{F}_\sigma(\mathbf{k},\omega) = -\hat{G}_N(\mathbf{k},-\omega)\,\hat{\varphi}_\sigma(\mathbf{k},\omega)\,\hat{G}(\mathbf{k},\omega), \quad (37)$$

where we introduced the normal state GF

$$\hat{G}_N(\mathbf{k},\omega) = \Big(\omega\hat{\tau}_0 - \hat{\varepsilon}(\mathbf{k}) - \hat{M}(\mathbf{k},\omega)/\hat{Q}\Big)^{-1}, \quad (38)$$

and the superconducting gap function

$$\hat{\varphi}_\sigma(\mathbf{k},\omega) = \hat{\Delta}_\sigma(\mathbf{k}) + \hat{\Phi}_\sigma(\mathbf{k},\omega)/\hat{Q}. \quad (39)$$

To calculate the self-energy matrix (35) we use the mode-coupling approximation which is equivalent to the NCA in the diagram technique for GFs. In this approximation, a propagation of Fermi-like excitations described by the operator $X_l^{\sigma'2}$, and Bose-like excitations described by the operator $B_{i\sigma\sigma'}$ for $l \neq i$ is assumed to be independent. Therefore, the time-dependent multiparticle correlation functions in the self-energy operators (35) can be written as a product of fermionic and bosonic correlation functions,

$$\left\langle X_{l'}^{2\sigma''} B^\dagger_{j\sigma\sigma''} | B_{i\sigma\sigma'}(t) X_l^{\sigma'2}(t)\right\rangle = \delta_{\sigma',\sigma''}\left\langle X_{l'}^{2\sigma'} X_l^{\sigma'2}(t)\right\rangle \times \left\langle B^\dagger_{j\sigma\sigma'} | B_{i\sigma\sigma'}(t)\right\rangle, \quad (40)$$

$$\left\langle X_{l'}^{\bar{\sigma}''2} B_{j\bar{\sigma}\bar{\sigma}''} | B_{i\sigma\sigma'}(t) X_l^{\sigma'2}(t)\right\rangle = \delta_{\sigma',\sigma''}\left\langle X_{l'}^{\bar{\sigma}'2} X_l^{\sigma'2}(t)\right\rangle \times \left\langle B_{j\bar{\sigma}\bar{\sigma}'} B_{i\sigma\sigma'}(t)\right\rangle. \quad (41)$$

The time-dependent correlation functions are calculated self-consistently using the corresponding GFs.

In particular, the normal and anomalous diagonal components of the self-energy for the two-hole subband are determined by the expressions

$$M^{22}(\mathbf{k},\omega) = \frac{1}{N}\sum_{\mathbf{q}}\int_{-\infty}^{+\infty} dz\, K^{(+)}(\omega,z|\mathbf{q},\mathbf{k}-\mathbf{q}) \times \left\{-\frac{1}{\pi}\mathrm{Im}\left[G^{22}(\mathbf{q},z) + G^{11}(\mathbf{q},z)\right]\right\}, \quad (42)$$

$$\Phi^{22}_\sigma(\mathbf{k},\omega) = \frac{1}{N}\sum_{\mathbf{q}}\int_{-\infty}^{+\infty} \mathrm{d}z\, K^{(-)}(\omega,z|\mathbf{q},\mathbf{k}-\mathbf{q}) \times \left\{-\frac{1}{\pi}\mathrm{Im}\left[F^{22}_\sigma(\mathbf{q},z) - F^{11}_\sigma(\mathbf{q},z)\right]\right\}, \quad (43)$$

where $G^{\alpha\alpha}(\mathbf{q},z)$ and $F^{\alpha\alpha}_\sigma(\mathbf{q},z)$ are given by the diagonal components of the matrices (36), (37). Similar expressions hold for the self-energy components $M^{11}(\mathbf{k},\omega)$ and $\Phi^{11}_\sigma(\mathbf{k},\omega)$ for electron doping when the Fermi energy located in the one-hole subband (see Ref. [40]). Note, that in the paramagnetic normal state the GF (36) and the self-energy (42) do not depend on the spin σ.

The kernel of the integral equations (42) and (43) has a form, similar to the strong-coupling Migdal-Eliashberg theory [41–44]:

$$K^{(\pm)}(\omega,z|\mathbf{q},\mathbf{k}-\mathbf{q}) = \frac{1}{\pi}\int_{-\infty}^{+\infty}\mathrm{d}\Omega\,\frac{1+N(\Omega)-n(z)}{\omega - z - \Omega} \times \Big\{|t(\mathbf{q})|^2\mathrm{Im}\chi_{sf}(\mathbf{k}-\mathbf{q},\Omega) \pm |g(\mathbf{k}-\mathbf{q})|^2\mathrm{Im}\chi_{ph}(\mathbf{k}-\mathbf{q},\Omega) \pm \left[|V(\mathbf{k}-\mathbf{q})|^2 + |t(\mathbf{q})|^2/4\right]\mathrm{Im}\,\chi_{cf}(\mathbf{k}-\mathbf{q},\Omega)\Big\}, \quad (44)$$

where $n(\omega) = [e^{\omega/T}+1]^{-1}$ and $N(\omega) = [e^{\omega/T}-1]^{-1}$. The spectral densities of bosonic excitations are determined by the dynamic susceptibility for spin (sf), number (charge) (cf), and lattice (phonon) (ph) fluctuations

$$\chi_{sf}(\mathbf{q},\omega) = -\langle\langle \mathbf{S}_\mathbf{q}|\mathbf{S}_{-\mathbf{q}}\rangle\rangle_\omega, \quad (45)$$

$$\chi_{cf}(\mathbf{q},\omega) = -\langle\langle \delta N_\mathbf{q}|\delta N_{-\mathbf{q}}\rangle\rangle_\omega, \quad (46)$$

$$\chi_{ph}(\mathbf{q},\omega) = -\langle\langle u_\mathbf{q}|u_{-\mathbf{q}}\rangle\rangle_\omega, \quad (47)$$

which are defined in terms of the commutator GFs [36,37] for the spin $\mathbf{S}_\mathbf{q}$, number $\delta N_\mathbf{q} = N_\mathbf{q} - \langle N_\mathbf{q}\rangle$, and lattice displacement (phonon) $u_\mathbf{q}$ operators.

In the NCA, vertex corrections are neglected as in the Migdal-Eliashberg theory. For the EPI $g(\mathbf{k}-\mathbf{q})$ the vertex corrections are small, as shown by Migdal [41]. The interaction $t(\mathbf{q})$ with spin-fluctuations (45) induced by the intraband hopping is not small and vertex corrections may be important. However, as was shown in reference [45] a certain set of diagrams, in particular the first crossing diagram, vanishes due to kinematic restrictions for spin scattering processes. Moreover, in reference [46] it was found that the renormalization of the vertex for a short AF correlation length is weak. Therefore, the NCA for the self-energy calculated self-consistently can be considered as a reasonable approximation. This approximation makes it possible to consider the strong coupling regime which is essential in study of renormalization of quasiparticle spectra and the superconducting pairing.

3.3 Two-subband model

In this section we derive a self-consistent system of equations for the GFs (36)–(38) and the self-energy components (42) and (43) for the two Hubbard subbands adopting several approximations to make the system of equations numerically tractable.

At first we consider equations for the normal state. The diagonal components of the GF (38) can be written as [30]:

$$G_N^{11(22)}(\mathbf{k},\omega) = [1-b(\mathbf{k})]G_{1(2)}(\mathbf{k},\omega) + b(\mathbf{k})G_{2(1)}(\mathbf{k},\omega), \quad (48)$$

$$G_{1(2)}(\mathbf{k},\omega) = \frac{1}{\omega - \varepsilon_{1(2)}(\mathbf{k}) - \Sigma(\mathbf{k},\omega)}, \quad (49)$$

where the hybridization parameter $b(\mathbf{k}) = [\varepsilon_2(\mathbf{k}) - \omega_2(\mathbf{k})]/[\varepsilon_2(\mathbf{k}) - \varepsilon_1(\mathbf{k})]$. The self-energy can be approximated by the same function for the both subbands,

$$\Sigma(\mathbf{k},\omega) = \frac{1}{N}\sum_{\mathbf{q}}\int_{-\infty}^{+\infty} dz\, K^{(+)}(\omega,z|\mathbf{q},\mathbf{k}-\mathbf{q}) \times [-(1/\pi)]\,\mathrm{Im}\,[G_1(\mathbf{q},z) + G_2(\mathbf{q},z)]. \quad (50)$$

The chemical potential μ is calculated from the equation for the average hole occupation number (6):

$$n = 1+\delta = 2\langle X_i^{\sigma\sigma}\rangle + 2\langle X_i^{22}\rangle = \frac{2}{N}\sum_{\mathbf{q}} N_h(\mathbf{q}), \quad (51)$$

where the hole occupation number is given by

$$N_{(h)}(\mathbf{k}) = N_{(h1)}(\mathbf{k}) + N_{(h2)}(\mathbf{k}), \quad (52)$$
$$N_{(h1)}(\mathbf{k}) = [Q_1 + (n-1)b(\mathbf{k})]\,N_1(\mathbf{k}),$$
$$N_{(h2)}(\mathbf{k}) = [Q_2 - (n-1)b(\mathbf{k})]\,N_2(\mathbf{k}),$$
$$N_{1(2)}(\mathbf{k}) = -\frac{1}{\pi}\int_{-\infty}^{\infty}\frac{d\omega}{e^{\omega/T}+1}\,\mathrm{Im}\,G_{1(2)}(\mathbf{k},\omega). \quad (53)$$

Density of states (DOS) is determined by

$$A(\omega) = \frac{1}{N}\sum_{\mathbf{k}} A_{(h)}(\mathbf{k},\omega), \quad (54)$$

where the spectral function for holes reads

$$A_{(h)}(\mathbf{k},\omega) = [Q_1 + P(\mathbf{k})]A_1(\mathbf{k},\omega) + [Q_2 - P(\mathbf{k})]A_2(\mathbf{k},\omega), \quad (55)$$
$$A_{1(2)}(\mathbf{k},\omega) = -(1/\pi)\,\mathrm{Im}G_{1(2)}(\mathbf{k},\omega).$$

Here the hybridization parameter $P(\mathbf{k}) = (n-1)b(\mathbf{k}) - 2\sqrt{Q_1 Q_2}\,[W(\mathbf{k})/\Lambda(\mathbf{k})]$ takes into account contributions from both the diagonal and off-diagonal components of the GF (38).

Now we formulate equations for the superconducting gap (39). We consider the case of hole doping when the Fermi energy is located in the two-hole subband, $n = 1+\delta > 1$. By taking into account the gap equation (34) in the MFA and the self-energy (43), equation (39) for the two-hole subband gap $\varphi(\mathbf{k},\omega) = \sigma\varphi_{2,\sigma}(\mathbf{k},\omega)$ reads,

$$\varphi(\mathbf{k},\omega) = \frac{1}{N}\sum_{\mathbf{q}}\int_{-\infty}^{+\infty} dz\,\left[-\frac{\sigma}{\pi Q_2}\mathrm{Im}F_\sigma^{22}(\mathbf{q},z)\right] \times\left\{[J(\mathbf{k}-\mathbf{q}) - V(\mathbf{k}-\mathbf{q})]\,\frac{1}{2}\tanh\frac{z}{2T} + K^{(-)}(\omega,z|\mathbf{q},\mathbf{k}-\mathbf{q})\right\}. \quad (56)$$

Here the contribution from the one-hole subband $F_\sigma^{11}(\mathbf{q},z)$ in (43) was neglected since this filled band much below the Fermi level gives a vanishingly small contribution to the pairing. To determine the superconducting T_c it is sufficient to solve a linear equation for the gap (56) using the linear approximation for the pair GF (37),

$$F_\sigma^{22}(\mathbf{k},\omega) = -G_N^{22}(\mathbf{k},-\omega)G_N^{22}(\mathbf{k},\omega)\,\sigma\varphi(\mathbf{k},\omega)Q_2 \approx -[1-b(\mathbf{q})]^2\,G_2(\mathbf{k},-\omega)G_2(\mathbf{k},\omega)\,\sigma\varphi(\mathbf{k},\omega)Q_2. \quad (57)$$

As in (56), here we neglect the GF $G_1(\mathbf{k},\omega)$ in (48) since the contribution to the pairing from the one-hole subband much below the Fermi energy is small.

For numerical calculations, it is convenient to introduce the imaginary frequency representation, $i\omega_n = i\pi T(2n+1)$, $n = 0, \pm1, \pm2, \ldots$ In this representation the self-energy (50) reads

$$\Sigma(\mathbf{k},\omega_n) = -\frac{T}{N}\sum_{\mathbf{q}}\sum_m \lambda^{(+)}(\mathbf{q},\mathbf{k}-\mathbf{q}\mid\omega_n-\omega_m) \times [G_1(\mathbf{q},\omega_m) + G_2(\mathbf{q},\omega_m)] \equiv i\omega_n\,[1-Z(\mathbf{k},\omega_n)] + X(\mathbf{k},\omega_n). \quad (58)$$

Here we introduced the renormalization parameters

$$\omega\,[1-Z(\mathbf{k},\omega)] = (1/2)\,[\Sigma(\mathbf{k},\omega) - \Sigma(\mathbf{k},-\omega)], \quad (59)$$
$$X(\mathbf{k},\omega) = (1/2)\,[\Sigma(\mathbf{k},\omega) + \Sigma(\mathbf{k},-\omega)]. \quad (60)$$

The normal GF (49) for the two subbands takes the form:

$$\{G_{1(2)}(\mathbf{k},\omega_n)\}^{-1} = i\omega_n - \varepsilon_{1(2)}(\mathbf{k}) - \Sigma(\mathbf{k},\omega_n) = i\omega_n Z(\mathbf{k},\omega_n) - [\varepsilon_{1(2)}(\mathbf{k}) + X(\mathbf{k},\omega_n)]. \quad (61)$$

The hole occupation number (53) in terms of the GF (61) reads:

$$N_{1(2)}(\mathbf{k}) = \frac{1}{2} + T\sum_m G_{1(2)}(\mathbf{k},\omega_m). \quad (62)$$

The gap equation (56) in the linear approximation for the pair GF (57) can be written as

$$\varphi(\mathbf{k},\omega_n) = \frac{T_c}{N}\sum_{\mathbf{q}}\sum_m \{\,J(\mathbf{k}-\mathbf{q}) - V(\mathbf{k}-\mathbf{q}) + \lambda^{(-)}(\mathbf{q},\mathbf{k}-\mathbf{q}\mid\omega_n-\omega_m)\} \times \frac{[1-b(\mathbf{q})]^2\,\varphi(\mathbf{q},\omega_m)}{[\omega_m Z(\mathbf{q},\omega_m)]^2 + [\varepsilon_2(\mathbf{q}) + X\mathbf{q},\omega_m)]^2}. \quad (63)$$

The interaction functions in (58) and (63) in the imaginary frequency representation are given by

$$\lambda^{(\pm)}(\mathbf{q},\mathbf{k}-\mathbf{q}|\nu_n) = -|t(\mathbf{q})|^2\,\chi_{sf}(\mathbf{k}-\mathbf{q},\nu_n) \mp \{\,[|V(\mathbf{k}-\mathbf{q})|^2 + |t(\mathbf{q})|^2/4] \times \chi_{cf}(\mathbf{k}-\mathbf{q},\nu_n) + |g(\mathbf{k}-\mathbf{q})|^2 \times \chi_{ph}(\mathbf{k}-\mathbf{q},\nu_n)\,\}. \quad (64)$$

Thus, we have derived the self-consistent system of equations for the normal GF (61), the self-energy (58), and the gap function (63).

4 Results and discussion

4.1 Model parameters

To perform numerical calculations we should specify model parameters in the derived system of equations. For the intersite CI $V(\mathbf{q})$ we consider two models. In the first model the CI is determined by the repulsion of two holes on the n.n. lattice sites,

$$V_1(\mathbf{q}) = 2V_1\,(\cos q_x + \cos q_y). \quad (65)$$

According to the cell-perturbation method [32], for the conventional values of electronic parameters in the p-d model for the CuO_2 plane, the CI of two n.n. holes is estimated by the value $V_1 = 0.1$–0.2 eV. The CI for n.n.n. holes, $4\,V_2\,\cos q_x \cos q_y$, is much smaller, $V_2/V_1 \sim 0.04$ and can be safely neglected.

As the second model we consider the 2D screened CI suggested in reference [22]:

$$V_c(\mathbf{q}) = \frac{2\pi e^2}{a\,\epsilon_0}\frac{1}{a|\mathbf{q}| + a\kappa} \equiv u_c\,\frac{1}{a|\mathbf{q}| + a\kappa}, \quad (66)$$

where a is the lattice parameter (below we put $a = 1$) and the dielectric constant ϵ_0 takes into account lattice polarization induced by ligand fields. We assume that the screening parameter κ depends on the doping and can be described by the interpolation formula: $a\kappa = 4\delta$, so that $a\kappa = 0.2$ in the underdoped case ($\delta = 0.05$) and $a\kappa = 1$ for the overdoped case ($\delta = 0.25$). The energy u_c we estimate from calculation of the CI (66) at $\kappa = 0$ for two n.n. holes at the distance a_x assuming it to be equal to V_1 in the model (65): $V_{c1}(\kappa = 0) = (u_c/N)\sum_{\mathbf{q}}(\cos q_x/q) = V_1$. From this equation we get an estimation $u_c = V_1/0.175 \approx 1$ eV or $u_c = 2.5t$ for $t = 0.4$ eV. Here for convenience, we take $V_1 = 0.175$ eV.

In the present study we do not perform self-consistent computation of spin and charge excitation spectra but adopt certain models for the spin (45), charge (46), and phonon (47) susceptibility in equation (44) or equation (64). Since we consider the electronic spectrum only in the normal state and calculate superconducting transition temperature T_c from the linearized gap equation (56) or (63), the feedback effects caused by opening a superconducting gap are not essential which justifies usage of model functions for the susceptibility.

Due to a large energy scale of charge fluctuations, of the order of several t, in comparison with the spin excitation energy of the order of J, the charge fluctuation contributions in equation (44) can be considered in the static limit:

$$\chi_{cf}(\mathbf{k}) = \chi_{cf,1}(\mathbf{k}) + \chi_{cf,2}(\mathbf{k}), \quad (67)$$
$$\chi_{cf,1(2)}(\mathbf{k}) = -\frac{1}{N}\sum_{\mathbf{q}}\frac{N_{h1(2)}(\mathbf{q}+\mathbf{k}) - N_{h1(2)}(\mathbf{q})}{\varepsilon_{1(2)}(\mathbf{q}+\mathbf{k}) - \varepsilon_{1(2)}(\mathbf{q})}$$

where the hole occupation numbers $N_{h1(2)}(\mathbf{q})$ are defined in equation (52). It is assumed that the system is far away from a charge instability or a stripe formation when the energy dependence of the charge susceptibility may be essential (see, e.g., Refs. [47–49]).

For the dynamical spin susceptibility $\chi_{sf}(\mathbf{q},\omega) = -\langle\langle \mathbf{S}_q \mid \mathbf{S}_{-q}\rangle\rangle_\omega$ we take a model suggested in numerical studies [50,51]:

$$\mathrm{Im}\,\chi_{sf}(\mathbf{q},\omega + i0^+) = \chi_{sf}(\mathbf{q})\,\chi''_{sf}(\omega) = \frac{\chi_Q}{1+\xi^2[1+\gamma(\mathbf{q})]}\tanh\frac{\omega}{2T}\,\frac{1}{1+(\omega/\omega_s)^2}. \quad (68)$$

The $\mathbf{q}$-dependence in $\chi_{sf}(\mathbf{q})$ is determined by the AF correlation length ξ (in units of a). The frequency dependence is determined by a broad spin-fluctuation spectrum $\chi''_{sf}(\omega)$ with a cut-off energy of the order of the exchange energy $\omega_s \sim J$. This type of the spin-excitation spectrum was found also in the microscopic theory for the t-J model in reference [52]. The strength of the spin-fluctuation interaction given by the static susceptibility $\chi_Q = \chi_{sf}(\mathbf{Q})$ at the AF wave vector $\mathbf{Q} = (\pi,\pi)$,

$$\chi_Q = \frac{3(1-\delta)}{2\omega_s}\left\{\frac{1}{N}\sum_{\mathbf{q}}\frac{1}{1+\xi^2[1+\gamma(\mathbf{q})]}\right\}^{-1}, \quad (69)$$

is fixed by the normalization condition:

$$\frac{1}{N}\sum_{\mathbf{q}}\int_{-\infty}^{+\infty}\frac{d\omega}{\pi}\,N(\omega)\,\mathrm{Im}\chi_{sf}(\mathbf{q},\omega) = \langle \mathbf{S}_i^2\rangle = \frac{3}{4}(1-\delta).$$

Spin correlation functions C_1, C_2 (30) in the single-particle excitation spectrum (25) can be calculated using the same model (68):

$$C_1 = \frac{1}{N}\sum_{\mathbf{q}} C_{\mathbf{q}}\,\gamma(\mathbf{q}), \quad C_2 = \frac{1}{N}\sum_{\mathbf{q}} C_{\mathbf{q}}\,\gamma'(\mathbf{q}). \quad (70)$$

Here the spin correlation function $C_{\mathbf{q}} = \langle \mathbf{S}_{\mathbf{q}}\mathbf{S}_{-\mathbf{q}}\rangle = C(\xi)/\{1+\xi^2[1+\gamma(\mathbf{q})]\}$ where $C(\xi) = \chi_Q\,(\omega_s/2)$. The results of computation of the correlation functions at several values of the AF correlation length ξ related to the hole concentrations δ are given in Table 1 where the static susceptibility χ_Q and the projected spin susceptibility $\widehat{\chi}_{sf}$ (see Eq. (82)) are also given.

To estimate the contribution from phonons in equation (44) we consider a model susceptibility for optic

Table 1. Spin correlation functions C_1, C_2, spin susceptibility χ_Q, and projected spin susceptibility $\widehat{\chi}_{sf}$ for several values of AF correlation length ξ related to hole concentration δ.

ξ/a	δ	C_1	C_2	$\chi_Q\, t$	$-\widehat{\chi}_{sf}\, t$
3.4	0.05	– 0.26	0.16	29.5	1.32
2.4	0.10	– 0.20	0.11	12.6	1.05
1.5	0.25	– 0.12	0.05	6.8	0.61

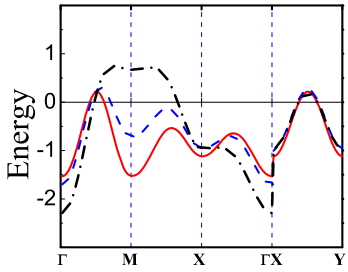

Fig. 1. (Color online) Electron dispersion in the MFA $\varepsilon_2(\mathbf{k})$ along the symmetry directions $\Gamma(0,0) \to M(\pi,\pi) \to X(\pi,0) \to \Gamma(0,0)$ and $X(\pi,0) \to Y(0,\pi)$ for $\delta = 0.05$ (red solid line), 0.10 (blue dashed line), and 0.25 (black dash-dotted line). Fermi energy for hole doping is at $\omega = 0$.

phonons and the EPI matrix element in the form similar to reference [53]:

$$V_{ep}(\mathbf{q},\omega) = |g(\mathbf{q})|^2 \chi_{ph}(\mathbf{q},\omega) = g_{ep}\, \frac{\omega_0^2}{\omega_0^2 - \omega^2}\, S(q), \quad (71)$$

where g_{ep} is the "bare" matrix element for the short-range EPI, while the momentum dependence of the EPI is determined by the vertex correction $S(q)$. It takes into account a strong suppression of charge fluctuations at small distances (large scattering momenta q) induced by electron correlations as proposed in reference [28]. For the vertex function we take the model

$$S(q) = \frac{1}{\kappa_1^2 + q^2} \equiv \frac{\xi_{ch}^2}{1 + \xi_{ch}^2\, q^2}, \quad (72)$$

where the charge correlation length $\xi_{ch} = 1/\kappa_1$ determines the radius of a "correlation hole". Taking into account that $\xi_{ch} \sim a/\delta$ [28], we can use the relation $\xi_{ch} = 1/(2\delta)$ in numerical computations. This gives $\xi_{ch} \simeq 10$ for the underdoped case ($\delta = 0.05$) and $\xi_{ch} \simeq 2$ for the overdoped case ($\delta = 0.25$). We assume a strong EPI $g_{ep} = 5\,t = 2.0$ eV and take $\omega_0 = 0.1\,t = 0.04$ eV.

In computations we use the following parameters for the model (1): $U = \Delta_{pd} = 8\,t$, $t' = -0.2\,t$, $t'' = 0.10\,t$. As an energy unit we use $t = 0.4$ eV. The exchange interaction is described by the function $J(\mathbf{q}) = 2J\,(\cos q_x + \cos q_y)$ with $J = 0.4t$. For the CI energy for the n.n. holes we take $V_1 = 0.44t$ and $u_c = 2.5t$. The electronic spectrum in the normal state is calculated at $T = 0.02t \sim 100$ K. In computations the grid of 64×64 (k_x, k_y) points and up to 1200 imaginary frequencies ω_n were used.

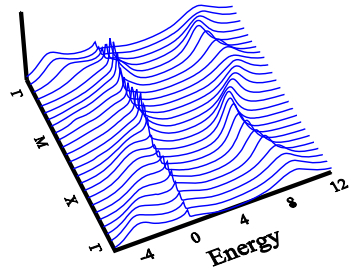

Fig. 2. Spectral function in the SCA along the symmetry directions $\Gamma(0,0) \to M(\pi,\pi) \to X(\pi,0) \to \Gamma(0,0)$ for hole concentration $\delta = 0.10$.

4.2 Electronic spectrum in the normal state

At first we consider results in the MFA for the electronic spectrum (25). The doping dependence of the electron dispersion for the two-hole subband $\varepsilon_2(\mathbf{k})$ along the symmetry directions in the 2D Brillouin zone (BZ) is shown in Figure 1. For small doping, $\delta = 0.05$, the energy at the $M(\pi,\pi)$ and $\Gamma(0,0)$ points are nearly equal as in the AF long-range order state. Only small hole-like FS pockets close to the $(\pm\pi/2, \pm\pi/2)$ points emerge at this doping. With increasing doping, the AF correlation length decreases that results in increasing of the electron energy at the $M(\pi,\pi)$ point and at some critical doping $\delta \sim 0.12$ a large FS appears. At the same time, the renormalized two-hole subband width increases with doping from $\widetilde{W} \approx 2\,t$ at $\delta = 0.05$ to $\widetilde{W} \approx 3\,t$ at $\delta = 0.25$, which, however, remains less than the "bare" Hubbard bandwidth $W = 4t\,(1+\delta)$ where short-range AF correlations are disregarded. Note that in the dynamical mean field theory (DMFT) this narrowing of the subbands due to the short-range AF correlations is missed [54,55], while they are taken into account partly in the cluster DMFT [56]. However, as shown in the DMFT the self-energy contribution strongly renormalizes the electronic spectrum found in the MFA.

To consider the self-energy effects in the electronic spectrum, a strong coupling approximation (SCA) should be considered by a self-consistent solution of the system of equations for the normal GF (49) and the self-energy (50). In reference [30] a detailed investigation of the normal state electronic spectrum for the conventional Hubbard model in SCA was performed. Therefore, here we present only the results of the electronic spectrum computation for the model (1) which are important for further studies of superconductivity in the model. The spectral functions (55) along the symmetry directions are presented in Figures 2 and 4 for $\delta = 0.10$ and $\delta = 0.25$, respectively. The dispersion curves given by the maximum of the spectral function (55) at the same doping are displayed in Figures 3 and 5.

In comparison with the MFA in Figure 1, a rather flat energy dispersion is found with QP peaks at the FS. In general, strong increase of the dispersion and intensity of the QP peaks is observed in the overdoped region in comparison with the underdoped region. This is in agreement with our detailed studies of temperature and doping dependence of the self-energy (50) and spectral function (55)

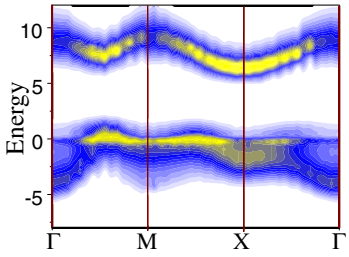

Fig. 3. (Color online) Electron dispersion curves in the SCA along the symmetry directions $\Gamma(0,0) \rightarrow M(\pi,\pi) \rightarrow X(\pi,0) \rightarrow \Gamma(0,0)$ for hole concentration $\delta = 0.10$.

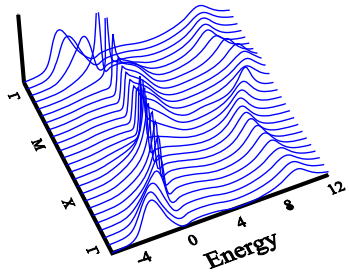

Fig. 4. The same as in Figure 2 for hole concentration $\delta = 0.25$.

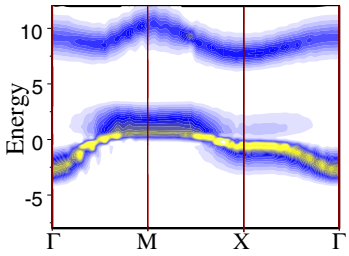

Fig. 5. (Color online) The same as in Figure 3 for hole concentration $\delta = 0.25$.

in [30] which have proved strong influence of AF spin-correlations on the spectra.

To estimate the coupling constant $\lambda(\mathbf{q})$ in the two-hole subband, we calculated the renormalization parameter $Z(\mathbf{q})$ (59) at the Fermi energy,

$$Z(\mathbf{q}) = Z(\mathbf{q}, \omega = 0) = 1 + \lambda(\mathbf{q}) = 1 - [\, d\,\mathrm{Re}\,\Sigma(\mathbf{q},\omega)/d\omega]|_{\omega=0}. \quad (73)$$

The doping dependence of $Z(\mathbf{q})$ is shown in Figure 6. It weakly depends on δ in the underdoped case for $\delta \lesssim 0.15$ but sharply decreases in the overdoped case for $\delta \gtrsim 0.25$. The temperature dependence of $Z(\mathbf{q})$ presented in Figure 7 is weak at temperatures lower than the characteristic energy of spin fluctuations $\omega_s \sim J$. The EPI gives a small contribution to the coupling constant as follows from the comparison of $Z(\mathbf{q})$ induced by both spin-fluctuations and EPI contributions (red solid line in Fig. 7) with the contribution caused only by spin-fluctuations (blue dashed line). The renormalization parameter $X(\mathbf{q})$ (60) at the Fermi energy

$$X(\mathbf{q}) = X(\mathbf{q}, \omega = 0) = \mathrm{Re}\Sigma(\mathbf{q}, 0), \quad (74)$$

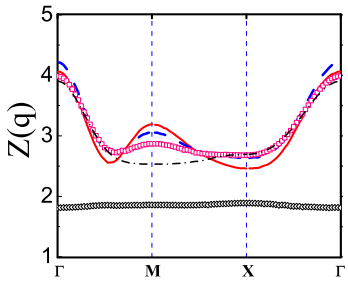

Fig. 6. (Color online) Doping dependence of the renormalization parameter $Z(\mathbf{q})$ along the symmetry directions $\Gamma(0,0) \rightarrow M(\pi,\pi) \rightarrow X(\pi,0) \rightarrow \Gamma(0,0)$ at $T \approx 140$ K for $\delta = 0.05$ (red solid line), $\delta = 0.10$ (blue dashed line), $\delta = 0.15$ (pink squares), $\delta = 0.25$ (black dash-dotted line), and $\delta = 0.35$ (black diamonds).

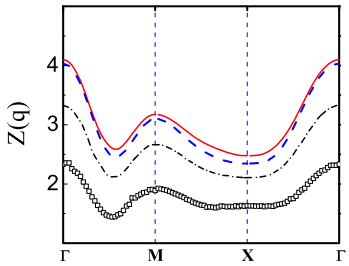

Fig. 7. (Color online) Temperature dependence of the renormalization parameter $Z(\mathbf{q})$ for $\delta = 0.05$ at $T \approx 140$ K (red solid line), $T \approx 580$ K (black dash-dotted line), and $T \approx 1100$ K (black squares). Blue dashed line shows $Z(\mathbf{q})$ for $\delta = 0.05$ caused only by the spin-fluctuation contribution.

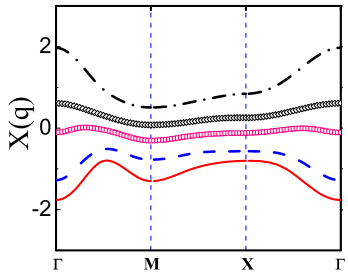

Fig. 8. (Color online) Doping dependence of the parameter $X(\mathbf{q})$. Notation are the same as in Figure 6.

which determines the shift of the dispersion curve is plotted along the symmetry directions in Figure 8. $X(\mathbf{q})$ decreases with doping in the underdoped region as $Z(\mathbf{q})$, but in the overdoped region reveals an irregular behavior and becomes small at large doping as $Z(\mathbf{q})$. These results demonstrate that at large doping both the electron interaction with spin-fluctuations and the EPI become weak.

4.3 Superconducting gap and T_c

For a comparison of various contributions to the superconducting gap equation (56), as the first step, we consider a weak-coupling approximation (WCA). In the WCA, the interaction (44) is approximated by its value close to the

Fermi energy, $|\omega, z| \sim 0$. Then integration over Ω of the dynamical susceptibility in (44) yields

$$\int_{-\infty}^{+\infty} \frac{d\Omega}{\pi} \frac{\mathrm{Im}\,\chi(\mathbf{q},\Omega)}{\omega - z - \Omega} \simeq \int_{-\infty}^{+\infty} \frac{d\Omega}{\pi} \frac{\mathrm{Im}\,\chi(\mathbf{q},\Omega)}{-\Omega} = -\chi(\mathbf{q}), \quad (75)$$

where $\chi(\mathbf{q}) = \mathrm{Re}\,\chi(\mathbf{q}, \Omega = 0)$ is the static susceptibility. In the WCA the self-energy contribution in the normal-state GF (49) is neglected that results in the BCS-type equation for the gap function at the Fermi energy $\varphi(\mathbf{k}) = \sigma\,\varphi_{2,\sigma}(\mathbf{k}, \omega = 0)$:

$$\varphi(\mathbf{k}) = \frac{1}{N}\sum_{\mathbf{q}} [1 - b(\mathbf{q})]^2 \frac{\varphi(\mathbf{q})}{2E(\mathbf{q})} \tanh\frac{E(\mathbf{q})}{2T} \big\{ J(\mathbf{k}-\mathbf{q}) - V(\mathbf{k}-\mathbf{q}) + \big[(1/4)|t(\mathbf{q})|^2 + |V(\mathbf{k}-\mathbf{q})|^2\big] \times \chi_{cf}(\mathbf{k}-\mathbf{q}) + |g(\mathbf{k}-\mathbf{q})|^2 \chi_{ph}(\mathbf{k}-\mathbf{q})\theta(\omega_0 - |\varepsilon_2(\mathbf{q})|) - |t(\mathbf{q})|^2\, \chi_{sf}(\mathbf{k}-\mathbf{q})\theta(\omega_s - |\varepsilon_2(\mathbf{q})|)\big\}, \quad (76)$$

where $E(\mathbf{q}) = [\varepsilon_2^2(\mathbf{q}) + |\varphi(\mathbf{q})|^2]^{1/2}$. Whereas for the exchange interaction and CI there are no retardation effects and the pairing occurs for all electrons in the two-hole subband, the EPI and spin-fluctuation contributions are restricted to the range of energies $\pm\omega_0$ and $\pm\omega_s$, respectively, near the FS, as determined by the θ-functions.

To estimate various contributions in the gap equation (76) we consider a model d-wave gap function, $\varphi(\mathbf{k}) = (\Delta/2)\,\eta(\mathbf{k})$ where $\eta(\mathbf{k}) = (\cos k_x - \cos k_y)$. Then the gap equation can be written in the form:

$$1 = \frac{1}{N}\sum_{\mathbf{q}} [1 - b(\mathbf{q})]^2 \frac{\eta(\mathbf{q})^2}{2E_{\mathbf{q}}} \tanh\frac{E_{\mathbf{q}}}{2T} \big\{ J - \widehat{V}_c + \widehat{V}_{cf} + (1/4)\,|t(\mathbf{q})|^2 \widehat{\chi}_{cf} + \widehat{V}_{ep}\,\theta(\omega_0 - |\varepsilon_2(\mathbf{q})|) - |t(\mathbf{q})|^2\,\widehat{\chi}_{sf}\theta(\omega_s - |\varepsilon_2(\mathbf{q})|)\big\}. \quad (77)$$

In this equation only $l = 2$ components of the static susceptibility and CI give contributions

$$\widehat{V}_c = \frac{1}{N}\sum_{\mathbf{k}} V(\mathbf{k}) \cos k_x, \quad (78)$$

$$\widehat{V}_{cf} = \frac{1}{N}\sum_{\mathbf{k}} |V(\mathbf{k})|^2 \chi_{cf}(\mathbf{k})\, \cos k_x, \quad (79)$$

$$\widehat{\chi}_{cf} = \frac{1}{N}\sum_{\mathbf{k}} \chi_{cf}(\mathbf{k}) \cos k_x, \quad (80)$$

$$\widehat{V}_{ep} = \frac{g_{ep}}{N}\sum_{\mathbf{k}} S(\mathbf{k}) \cos k_x, \quad (81)$$

$$\widehat{\chi}_{sf} = \frac{1}{N}\sum_{\mathbf{k}} \chi_{sf}(\mathbf{k}) \cos k_x. \quad (82)$$

Computation yields the following parameters for the n.n. intersite CI (65): $\widehat{V}_c = V_1 = 0.44t \approx 0.18$ eV. For the screened CI (66) we have:

$$\widehat{V}_c(\kappa) = \frac{u_c}{N}\sum_{\mathbf{q}} \frac{\cos q_x}{q + \kappa}, \quad (83)$$

where $\widehat{V}_c(\kappa) = 0.12\,t\ (0.28\,t) \approx 0.05\ (0.11)$ eV for $\kappa = 1\,(0.2)$, respectively (see Tab. 2). Note, that the projected CI (83) is much smaller than the CI energy $V_{c0}(\kappa) = (u_c/N)\sum_{\mathbf{q}}[1/(q + \kappa)]$. In particular, $\widehat{V}_c(\kappa)/V_{c0}(\kappa) = 0.15\ (0.24)$ for $\kappa = 1\,(0.2)$, respectively. In the conventional BCS theory the CI is suppressed by retardation effects described by large Bogoliubov-Morel logarithm, $\ln(\mu/\omega_{ph})$. In the Hubbard model there are no retardation effects for the AF exchange interaction but a reduction of the CI contribution is due to the d-wave pairing.

To estimate contributions from the charge fluctuations we use the static charge susceptibility (67). Applying this approximation to the screened CI (66) we get the following expression for charge contribution (79):

$$\widehat{V}_{cf}(\kappa) = \frac{u_c^2}{N}\sum_{\mathbf{k}} \frac{1}{(k + \kappa)^2}\, \chi_{cf}(\mathbf{k})\, \cos k_x, \quad (84)$$

where $\widehat{V}_{cf}(\kappa) = 0.05\ (0.25)\,t \approx 0.02\ (0.1)$ eV for $\kappa = 1\,(0.2)$, respectively. This contribution is smaller than the CI repulsion $\widehat{V}_c$ (83) and in our approximation the d-wave pairing induced by the screened CI in the second order $\widehat{V}_{cf}$ is destroyed by CI repulsion in the first order $\widehat{V}_c$ as was pointed out in reference [22]. The charge fluctuation contribution from the n.n. intersite CI (65) is even smaller, $\widehat{V}_{cf}^{nn} \approx 4 \times 10^{-3}\,t$. The contribution from the charge fluctuations (80) calculated for the static susceptibility (67) is also small: $\widehat{\chi}_{cf}(\delta) = (1/t)\,0.15 \times 10^{-2}\ (1.3 \times 10^{-2})$ for the hole concentrations $\delta = 0.05\ (0.10)$, respectively. For the averaged over the BZ vertex $\overline{|t(\mathbf{q})|^2} = (1/N)\sum_{\mathbf{q}} |t(\mathbf{q})|^2 \simeq 4\,t^2$ this contribution is equal to $\overline{|t(\mathbf{q})|^2}\,\widehat{\chi}_{cf} \lesssim 0.02$ eV and can be neglected.

The EPI contribution (81) is given by

$$\widehat{V}_{ep} = \frac{g_{ep}}{N}\sum_{\mathbf{k}} \frac{\xi_{ch}^2}{1 + \xi_{ch}^2\, k^2} \cos k_x \equiv g_{ep}\, S_d(\xi_{ch}), \quad (85)$$

where $S_d(\xi_{ch}) = 0.154\,(0.393)$ for $\xi_{ch} = 2\,(10)$, respectively. Thus, even for a strong EPI coupling $g_{ep} = 5t = 2$ eV we obtain a moderate contribution from the EPI for the d-wave pairing: $\widehat{V}_{ep}(\xi_{ch}) = 0.76\,t\,(1.96\,t) \approx 0.3\,(0.8)$ eV for $\xi_{ch} = 2\,(10)$, respectively. The EPI contribution to the s-wave pairing is given by the $l = 0$ component $S_0 = (1/N)\sum_{\mathbf{q}} S(q) = 0.31\ (0.57)$ for $\xi_{ch} = 2\ (10)$, respectively. The ratio of the d-wave S_d and the s-wave $S_s = S_0$ components of the EPI matrix elements is equal to $(S_d/S_0) = 0.43\ (0.60)$ for $\xi_{ch} = 2\ (10)$, respectively. This shows that at small hole concentrations δ (large charge correlation lengths $\xi_{ch} = 1/2\delta$) the EPI for the both components are comparable, while for the overdoped case the d-wave component S_d becomes considerably smaller than the s-wave component in agreement with the results of reference [28].

The spin-fluctuation contribution $\widehat{\chi}_{sf}$ calculated for the model $\chi_{sf}(\mathbf{q})$ in equation (68) for several values of the AF correlation length ξ is given in Table 1. Using the averaged over BZ vertex $\overline{|t(\mathbf{q})|^2} \simeq 4\,t^2$, we can

Table 2. CI parameters $\widehat{V}_c$, V_{c0}, $\widehat{V}_{cf}$, and EPI parameter $\widehat{V_{ep}}$ for several values of the CI screening constant $\kappa = 4\delta$ and the charge correlation length $\xi_{cf} = 1/2\delta$ for EPI related to hole concentration δ.

δ	κ	ξ_{cf}	$\widehat{V}_c/t$	V_{c0}/t	$\widehat{V}_{cf}/t$	$\widehat{V_{ep}}/t$
0.05	0.2	10	0.28	1.18	0.25	1.96
0.10	0.4	5	0.22	1.05	0.26	1.4
0.25	1	2	0.12	0.80	0.05	0.76

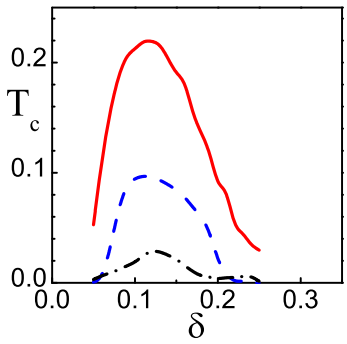

Fig. 9. (Color online) $T_c(\delta)$ in the WCA induced by all interactions (red solid line) and only by the spin-fluctuation contribution $\widehat{\chi}_{sf}$(blue dashed line) or only by the EPI $\widehat{V}_{ep}$ (black dash-dotted line).

estimate an effective spin-fluctuation coupling constant as $g_{sf} \simeq -4\,t^2\,\widehat{\chi}_{sf} = 5.3\,(2.4)t \approx 2\,(1)$ eV for $\delta = 0.05\,(0.25)$, respectively. Thus, the spin-fluctuation contribution to the pairing in equation (77) appears to be the largest. Note, that g_{sf} is close to the spin-fluctuation coupling constant $\widetilde{U} \approx 1.6$ eV found in reference [14] from ARPES data.

In Table 2 we present the coupling parameters in the equation for T_c (77). In the MFA the pairing can be induced by the AF exchange interaction $J = 0.4t = 0.16$ eV which is comparable with the repulsion caused by the screened CI: $\widehat{V}_c = (0.05-0.11)$ eV or even smaller than the n.n. hole CI $V_1 = 0.175$ eV. Therefore, the superconducting pairing in the MFA for the t-J model (in particular, the RVB state [4,5]) is strongly suppressed (or even destroyed) by the intersite Coulomb repulsion.

To calculate doping dependence of T_c we solve equation (77) by taking into account the exchange interaction J, the Coulomb repulsion $\widehat{V}_c$, and the contributions from the self-energy in the WCA: $\widehat{V}_{ep}$, $\widehat{\chi}_{sf}$, and $\widehat{V}_{cf}$, neglecting the small contribution $\widehat{\chi}_{cf}$. Results of the calculation are shown in Figure 9. The highest $T_c \approx 0.2\,t$ is found when all the contributions are taken into account. The spin-fluctuation pairing results in superconducting $T_c^{sf} \approx 0.04\,t$ much larger than $T_c^{ep} \approx 0.01t$ mediated by the EPI. For the **k**-independent EPI ($S(\mathbf{k}) = 1$) as in the Holstein model, the d-wave pairing is absent. The doping dependence of T_c qualitatively agrees with experiments in cuprates but its value is an order of magnitude higher.

The high values for T_c found in the WCA are explained by neglecting the reduction of the quasiparticle weight caused by the self-energy effects in the gap equation (63).

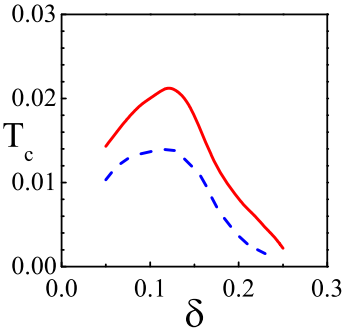

Fig. 10. (Color online) $T_c(\delta)$ induced by all interactions in equation (86) (red solid line) and only by spin-fluctuation contribution V_{sf} (blue dashed line).

It is convenient to write the gap equation in the form:

$$\varphi(\mathbf{k},\omega_n) = \frac{T_c}{N}\sum_{\mathbf{q}}\sum_{m}\big\{J(\mathbf{k}-\mathbf{q}) - V_c(\mathbf{k}-\mathbf{q}) - V_{sf}(\mathbf{q},\mathbf{k}-\mathbf{q},\omega_n-\omega_m) + V_{ep}(\mathbf{k}-\mathbf{q},\omega_n-\omega_m)\big\} \times \frac{[1-b(\mathbf{q})]^2\,\varphi(\mathbf{q},\omega_m)}{[\omega_m Z(\mathbf{q},\omega_m)]^2 + [\varepsilon_2(\mathbf{q}) + X(\mathbf{q},\omega_m)]^2}. \quad (86)$$

For $V_c(\mathbf{k}-\mathbf{q})$ we take the screened CI (66). Since the charge-fluctuations gives a much weaker contribution than the spin-fluctuation and electron-phonon interactions (see Tabs. 1 and 2), we neglect the term $[|V(\mathbf{k}-\mathbf{q})|^2 + |t(\mathbf{q})|^2/4]\,\chi_{cf}(\mathbf{k}-\mathbf{q},\nu_n)$ in the interaction function (64). Contributions induced by spin-fluctuations and the EPI are described by the functions

$$V_{sf}(\mathbf{q},\mathbf{k}-\mathbf{q},\omega_\nu) = |t(\mathbf{q})|^2\,\chi_{sf}(\mathbf{k}-\mathbf{q})F_{sf}(\omega_\nu), \quad (87)$$

$$V_{ep}(\mathbf{k}-\mathbf{q},\omega_\nu) = g_{ep}\,\frac{\omega_0^2}{\omega_0^2+\omega_\nu^2}\,S(\mathbf{k}-\mathbf{q}), \quad (88)$$

where the spectral function for spin fluctuations reads:

$$F_{sf}(\omega_\nu) = \frac{1}{\pi}\int_0^\infty \frac{2x\,dx}{x^2+(\omega_\nu/\omega_s)^2}\,\frac{\tanh(x\,\omega_s/2T)}{1+x^2}. \quad (89)$$

To calculate T_c and to find out the energy- and **k**-dependence of the gap $\varphi(\mathbf{k},\omega)$, equation (86) was solved by a direct diagonalization in (k_x, k_y, ω_n)-space. Since the largest contribution in equation (86) comes from energies close to the FS, we have used the renormalization parameters at the Fermi energy $Z(\mathbf{q})$ (73) and $X(\mathbf{q})$ (74) instead of the energy dependent ones. The results for $T_c(\delta)$ are shown in Figure 10. The highest $T_c \sim 0.021t \sim 100$ K is found when all the contributions are taken into account, though pairing induced only by spin-fluctuations also results in high $T_c^{sf} \sim 0.014t \sim 65$ K. The d-wave pairing induced only by the EPI is rather weak and is not displayed in Figure 10. The value of T_c is reduced by an order of magnitude in comparison with the WCA in Figure 9 due to a suppression of the QP weight by the factor $[1/Z(\mathbf{q})]^2$. The maximum value of T_c is found at lower value of doping $\delta_{opt} \approx 0.12$ than in experiments, $\delta_{opt}^{exp} = 0.16$.

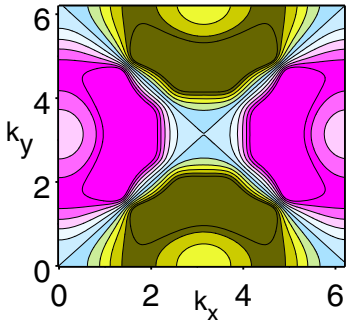

Fig. 11. (Color online) 2D plot of the SC gap $\varphi(\mathbf{k}, \omega \simeq 0)$.

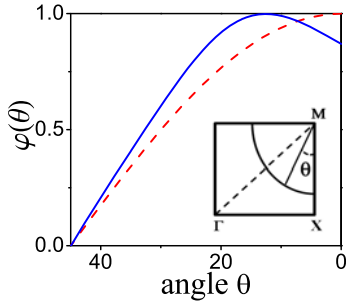

Fig. 12. (Color online) Angle dependence of the SC gap $\varphi(\theta)$ on the FS (blue bold line) in comparison with the model d-wave dependence $\varphi_d(\theta) = \cos 2\theta$ (red dashed lines).

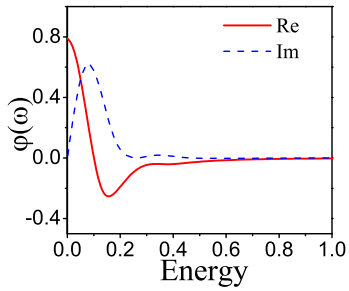

Fig. 13. Energy dependence of the real, Re $\varphi(\mathbf{k}, \omega)$, and imaginary, Im $\varphi(\mathbf{k}, \omega)$, parts of the SC gap in arbitrary units.

The $\mathbf{k}$-dependence of the gap function $\varphi(\mathbf{k}, \omega \simeq 0)$ at doping $\delta = 0.13$ for $(0 \leq k_x, k_y \leq 2\pi)$ is plotted in Figure 11. The gap reveals a distinct d-wave symmetry with maximum values in the vicinity of the FS. As shown in Figure 12, its angle dependence on the FS is close to the model d-wave dependence $\varphi_d(\theta) = \cos 2\theta$. Energy dependence (in units of t) of the gap function $\varphi(\mathbf{k}, \omega)$, the real and imaginary parts, is presented in Figure 13 at $\mathbf{k} \approx (0, \pi/2)$ and $\delta = 0.13$. Since the gap function was obtained as a solution of the linear equation at $T = T_c$ the value of the gap is given in arbitrary units. The energy variation of the gap occurs in the region of $\omega \lesssim 0.4t$, of the order of the characteristic spin-fluctuation energy $\omega_s = J = 0.4t$.

Generally, the results obtained in the SCA are in a qualitative agreement with experiments in the cuprate superconductors. They also demonstrate an important role of the self-energy effects in the normal and superconducting states in comparison with the MFA.

4.4 Comparison with previous theoretical studies

As briefly discussed in Section 1, various methods have been used in theoretical studies of superconductivity in the Hubbard model. Here we would like to emphasize our results in comparison with previous investigations of the problem.

At first we refer to results obtained in the weak or intermediate correlation limit. In particular, using the two-particle self-consistent non-perturbative approach (see, e.g., Refs. [57–61]) and the fluctuation-exchange (FLEX) approximation (see, e.g., Refs. [62,63] and reviews [8,9,64]), a system of equations was derived within the Fermi-liquid model to study self-consistently single-electron GFs and the spin and charge dynamical susceptibility. Within the FLEX approximation, the superconducting d-wave pairing was found in a narrow range of doping, very close to the AF instability. In our theory superconductivity is mediated by a broad spectrum of AF spin excitations (paramagnons) which results in the doping dependence of T_c close to experimentally observed (see Figs. 9, 10).

A general problem of the weak CI in the Hubbard model has been extensively studied within the RG approach (for reviews see Refs. [65,66]). The RG studies revealed a competition between various types of phases driven by electronic instability, such as the spin-density wave (SDW), charge-density wave (CDW), nematic (Pomeranchuk) phase, stripes, superconducting pairing, etc. (see reviews [67,68] and Refs. [69–73]). For a weak Hubbard interaction $U \sim t$ in a certain range of hopping parameters and doping the d-wave superconducting pairing can overcome other instabilities. An important role of the intersite Coulomb repulsion in the Hubbard model was found in reference [25], as mentioned in Section 1. In our theory we disregarded other instabilities and did not study a general phase diagram since it would demand investigation of a much more complicated system of equations which is beyond the scope of the present paper.

To consider cuprate superconductors, the strong correlation limit should be investigated. In many publications the spectrum of electronic excitations in the normal state in the Hubbard model was extensively studied. Here we refer to numerical simulations for finite clusters (see reviews [74–76]), the DMFT (see reviews [54,55]), the dynamical cluster approximation (DCA) [77–79] and the cluster DMFT (see, e.g., Refs. [56,80]). More accurate results have been obtained within the DCA and cluster DMFT methods where short-range AF correlations are partially taken into account. As we have pointed out in Sections 3.1 and 4.2, in our method short-range AF correlations are properly taken into consideration in the MFA resulting in a large reduction of the effective bandwidth $\widetilde{W}$. Consequently, a two-subband state in the Hubbard model is found even in the intermediate correlation limit, $U \sim 4\,t$. The spectral density computed in SCA

(Figs. 2 and 4), are in accord with numerical studies for the Hubbard model (see, e.g., Refs. [60,61,77,81,82]).

The most controversial problem is whether the superconductivity can emerge from the repulsion, as discussed in Section 1. Extensive numerical studies for finite clusters have revealed a tendency to the d-wave pairing in the Hubbard model, though a delicate balance between superconductivity and other instabilities (AF, SDW, CDW, etc.) was found (see, e.g., Refs. [75–80]). In reference [83], using the DCA with the quantum Monte Carlo method, the superconducting d-wave pairing and the isotope effect similar to observed in cuprates were found for the Hubbard-Holstein model. However, in several publications an appearance of the long-range superconducting order has not been confirmed (see, e.g., Ref. [84]). Therefore, analytical studies are desirable to elucidate this problem.

An accurate analytical method is based on the HO technique where the HO algebra is implemented rigorously. The superconducting pairing induced by the kinematic interaction for the HOs was first proposed by Zaitsev and Ivanov [85–87] who studied the two-particle vertex equation by applying the diagram technique for HOs. The momentum-independent s-wave pairing was found in the lowest order diagram approximation equivalent to the MFA. However, this solution violates the HO kinematics and the t-J model should be used to obtain the d-wave pairing mediated by the AF superexchange interaction (see, e.g., Refs. [88–91]). In this respect we should point out that in many publications superconductivity in the t-J model was studied in the MFA (see, e.g., Refs. [88,89,92–94]). As we have shown in Section 4.3, the intersite Coulomb repulsion suppresses or even destroys superconductivity induced by the AF superexchange interaction in the MFA. In particular, in cuprates, a sufficiently strong n.n. hole repulsion $V_1 = 0.1-0.2$ [32] may be detrimental for the RVB state [4,5]. The same remark refers to the studies of superconductivity in the conventional Hubbard model in the MFA (see, e.g., Refs. [38,95–98]). Therefore, consideration of the spin-fluctuation pairing beyond the MFA is essential in description of superconductivity in cuprates as discussed in detail in Section 4.3.

In comparison with studies of the intersite Coulomb repulsion in the weak correlation limit in references [22,25], in the strong correlation limit the intersite Coulomb repulsion V_{ij} to some extent is compensated by the nonretarded superexchange interaction J_{ij} (see Eqs. (31), (32)) which is absent in the weak correlation limit. At the same time, even for a sufficiently large component V_{c0} of the CI V_{ij}, the contribution to the gap equation is given by a much smaller d-wave partial harmonic (83) and therefore is not so detrimental to superconductivity in comparison with the conventional s-wave momentum-independent pairing.

Studies of the spin-fluctuation d-wave pairing in the presence of the EPI have shown that depending on the symmetry, the EPI could enhance or suppress superconducting pairing (see, e.g., Refs. [99,100]). In reference [53] the d-wave pairing induced by both the spin-fluctuations and EPI in the model (71) within the FLEX approximation was considered. It was revealed that a momentum-independent EPI strongly suppresses T_c, while the EPI with strong forward scattering can enhance T_c. In our theory the strong spin-fluctuation pairing is induced by the kinematic interaction which is absent in the weak correlation limit as in FLEX approximation, and therefore, the EPI plays only a secondary role in the d-wave pairing. A strong EPI in polaronic effects observed in the oxygen isotope effect on the in-plane penetration depth in cuprates [101] may be irrelevant for the pairing mediated by the d-wave partial harmonic of the EPI [102] as confirmed by a weak isotope effect on T_c in the optimally doped cuprates.

5 Conclusion

In the paper the theory of superconducting pairing within the extended Hubbard model (1) in the limit of strong electron correlations is presented. Using the Mori-type projection technique we obtained a self-consistent system of equations for normal and anomalous (pair) GFs and for the self-energy calculated in the NCA. The theory is similar to the Migdal-Eliasberg strong-coupling approximation.

We can draw the following conclusions about the mechanism of pairing in the extended Hubbard model. Solution of the gap equation in the weak coupling approximation (76) shows that for the d-wave pairing the intersite Coulomb repulsion gives a small contribution determined by $l = 2$ harmonic of the interaction function $V(\mathbf{k}-\mathbf{q})$. However, it can be larger than the AF superexchange interaction $J(\mathbf{k}-\mathbf{q})$, and the RVB-type superconducting pairing can be destroyed.

Pairing induced by charge fluctuations $\chi_{ch}(\mathbf{k}-\mathbf{q})$ appears to be quite weak (outside the charge-instability region). We have found that the d-wave component of the EPI, even for the model of strong forward scattering [28] and a large fully symmetric s-wave component, turned out to be small. The largest contribution to the d-wave pairing comes from the electron interaction with spin fluctuations induced by strong kinematic interaction $|t(\mathbf{q})|^2$, so that the EPI plays a secondary role in achieving high-T_c.

It is important to point out that the superconducting pairing induced by the AF superexchange interaction and spin-fluctuation scattering are caused by the kinematic interaction characteristic of systems with strong correlations. These mechanisms of superconducting pairing are absent in the fermionic models (for a discussion, see Ref. [103]) and are generic for cuprates. The intersite Coulomb repulsion is not strong enough to destroy the d-wave pairing mediated by spin fluctuations. Therefore, we believe that the magnetic mechanism of superconducting pairing in the Hubbard model in the limit of strong correlations is a relevant mechanism of high-temperature superconductivity in the copper-oxide materials.

The authors would like to thank A.S. Alexandrov and V.V. Kabanov for valuable discussions. One of the authors (N.P.) is

grateful to the MPIPKS, Dresden, for the hospitality during his stay at the Institute, where a part of the present work has been done. Partial financial support by the Heisenberg–Landau Program of JINR is acknowledged.

Note added in proof. When this work was submitted, we became aware of references [104–106] which consider the extended Hubbard model with the intersite Coulomb repulsion V. The results of the references [104,106] show that the on-site repulsion U effectively enhances the d-wave pairing which survives for large values of V up to $V \sim U/2 \gg J$ (Ref. [106]). This observation supports our model of spin-fluctuation pairing due to the kinematic interaction which emerges only in the strong correlation limit. As long as the Coulomb repulsion V does not exceed the kinematic interaction of the order of the kinetic energy, $V \lesssim 4\,t$, the d-wave pairing may survive. The small value of $V = J$ found in reference [105] is explained by application of the slave-boson representation in the MFA which ignores the kinematic interaction. We would like to thank A.-M.S. Tremblay for valuable discussion who drew our attention to those papers.

References

1. J.G. Bednorz, K.A. Müller, Z. Phys. B. **64**, 189 (1986)
2. *Handbook of High-Temperature Superconductivity. Theory and Experiment*, edited by J.R. Schrieffer, J.S. Brooks (Springer-Verlag, New York, 2007), Chaps. 13−15
3. N.M. Plakida, *High-Temperature Cuprate Superconductors* (Springer-Verlag, Berlin, 2010), Vol. 166, Chap. 7
4. P.W. Anderson, Science **235**, 1196 (1987)
5. P.W. Anderson, *The Theory of Superconductivity in the High-T_c Cuprates* (Princeton University Press, Princeton, 1997)
6. D.J. Scalapino, Phys. Rep. **250**, 329 (1995)
7. P. Monthoux, D. Pines, Phys. Rev. B **49**, 4261 (1994)
8. T. Moriya, K. Ueda, Adv. Phys. **49**, 555 (2000)
9. T. Moriya, K. Ueda, Rep. Prog. Phys. **66**, 1299 (2003)
10. A.V. Chubukov, D. Pines, J. Schmalian, in *The Physics of Conventional and Unconventional Superconductors*, edited by K.H. Bennemann, J.B. Ketterson (Springer-Verlag, Berlin, 2004), Vol. I, p. 495
11. Ar. Abanov, A.V. Chubukov, J. Schmalian, Adv. Phys. **52**, 119 (2003)
12. Ar. Abanov, A.V. Chubukov, M.R. Norman, Phys. Rev. B **78**, 220507(R) (2008)
13. A.A. Kordyuk, V.B. Zabolotnyy, D.V. Evtushinsky, D.S. Inosov, T.K. Kim, B. Büchner, S.V. Borisenko, Eur. Phys. J. Special Topics **188**, 153 (2010)
14. T. Dahm, V. Hinkov, S.V. Borisenko, A.A. Kordyuk, V.B. Zabolotnyy, J. Fink, B. Büchner, D.J. Scalapino, W. Hanke, B. Keimer, Nat. Phys. **5**, 780 (2009)
15. Ph. Bourges, in *The Gap Symmetry and Fluctuations in High Temperature Superconductors*, edited by J. Bok, G. Deutscher, D. Pavuna, S.A. Wolf (Plenum Press, 1998), p. 349
16. M. Le Tacon, G. Ghiringhelli, J. Chaloupka, M. Moretti Sala, V. Hinkov, M.W. Haverkort, M. Minola, M. Bakr, K.J. Zhou, S. Blanco-Canosa, C. Monney, Y.T. Song, G.L. Sun, C.T. Lin, G.M. De Luca, M. Salluzzo, G. Khaliullin, T. Schmitt, L. Braicovich, B. Keimer, Nat. Phys. **7**, 725 (2011)
17. A.A. Vladimirov, D. Ihle, N.M. Plakida, Phys. Rev. B **85**, 224536 (2012)
18. M.L. Kulić, in *Lectures on Physics of Highly Correlated Electronic Systems VIII*, edited by A. Avella, F. Mancini, *AIP Conf. Proc.* (Melville, New York, 2004), Vol. 715, p. 75
19. E.G. Maksimov, M.L. Kulić, O.V. Dolgov, Adv. in Cond. Mat. Phys., DOI: 10.1155/2010/423725 (2010)
20. S. Raghu, S.A. Kivelson, D.J. Scalapino, Phys. Rev. B **81**, 224505 (2010)
21. J. Hubbard, Proc. Roy. Soc. A **276**, 238 (1963)
22. A.S. Alexandrov, V.V. Kabanov, Phys. Rev. Lett. **106**, 136403 (2011)
23. M.Yu. Kagan, D.V. Efremov, M.S. Marienko, V.S. Valkov. JETP Lett. **93**, 725 (2011)
24. D.V. Efremov, M.S. Marenko, M.A. Baranov, M.Yu. Kagan, J. Exp. Theor. Phys. **90**, 861 (2000)
25. S. Raghu, E. Berg, A.V. Chubukov, S.A. Kivelson, Phys. Rev. B **85**, 024516 (2012)
26. P. Fulde, *Electronic Correlations in Molecules and Solids* (Springer-Verlag, Berlin, 1995)
27. *Strongly Correlated Systems. Theoretical Methods*, edited by A. Avella, F. Mancini (Springer-Verlag, Berlin, 2012), Vol. 171
28. R. Zeyher, M.L. Kulić, Phys. Rev. B **53**, 2850 (1996)
29. H. Mori, Prog. Theor. Phys. **34**, 399 (1965)
30. N.M. Plakida, V.S. Oudovenko, JETP **104**, 230 (2007)
31. J. Hubbard, Proc. Roy. Soc. A **285**, 542 (1965)
32. L.F. Feiner, J.H. Jefferson, R. Raimondi, Phys. Rev. B **53**, 8751 (1996)
33. V.J. Emery, Phys. Rev. Lett. **58**, 2794 (1987)
34. C.M. Varma, S. Schmitt-Rink, E. Abrahams, Solid State Commun. **62**, 681 (1987)
35. F.C. Zhang, T.M. Rice, Phys. Rev. B **37**, 3759 (1988)
36. D.N. Zubarev, Usp. Fiz. Nauk **71**, 71 (1960) [Sov. Phys. Usp. **3**, 320 (1960)]
37. D.N. Zubarev, *Nonequilibrium Statical Thermodynamics* (Consultant Bureau, New-York, 1974)
38. Gh. Adam, S. Adam, J. Phys. A **40**, 11205 (2007)
39. N.M. Plakida, L. Anton, S. Adam, Gh. Adam, Zh. Exp. Theor. Fyz. **124**, 367 (2003) [JETP **97**, 331 (2003)]
40. N.M. Plakida, Physica C **282–287**, 1737 (1997)
41. A.B. Migdal, Zh. Eksp. Teor. Fiz. **34**, 1438 (1956) [Soviet Phys. JETP **7**, 996 (1958)]
42. G.M. Eliashberg, Zh. Eksp. Teor. Fiz. **38**, 966 (1960)
43. G.M. Eliashberg, Zh. Eksp. Teor. Fiz. **39**, 1437 (1960) [Soviet Phys. JETP **11**, 696 (1960)]
44. G.M. Eliashberg, Zh. Eksp. Teor. Fiz. **12**, 1000 (1960)
45. Z. Liu, E. Manousakis, Phys. Rev. B **45**, 2425 (1992)
46. P. Monthoux, Phys. Rev. B **55**, 15261 (1997)
47. F. Becca, M. Tarquini, M. Grilli, C. Di Castro, Phys. Rev. B **54**, 12 443 (1996)
48. C. Castellani, C. Di Castro, M. Grilli, J. Phys. Chem. Solids **59**, 1694 (1998)
49. T. Ekino, A.M. Gabovich, Mai Suan Li, M. Pękała, H. Szymczak, A.I. Voitenko, J. Phys.: Condens. Matter **23**, 385701 (2011)
50. J. Jaklič, P. Prelovšek, Phys. Rev. Lett. **74**, 3411 (1995)
51. J. Jaklič, P. Prelovšek, Phys. Rev. Lett. **75**, 1340 (1995)
52. A.A. Vladimirov, D. Ihle, N.M. Plakida, Phys. Rev. B **80**, 104425 (2009)
53. A.I. Lichtenstein, M.L. Kulić, Physica C **245**, 186 (1995)

54. A. Georges, G. Kotliar, W. Krauth, M. Rozenberg, Rev. Mod. Phys. **68**, 13 (1996)
55. G. Kotliar, S.Y. Savrasov, K. Haule, V.S. Oudovenko, O. Parcollet, C.A. Marianetti, Rev. Mod. Phys. **78**, 865 (2006)
56. K. Haule, G. Kotliar, Phys. Rev. B **76**, 104509 (2007)
57. Y. Vilk, A.-M. Tremblay, J. Phys. Chem. Solids **56**, 1769 (1995)
58. Y. Vilk, A.-M. Tremblay, J. Phys. I **7**, 1309 (1997)
59. Y. Vilk, L. Chen, A.-M. Tremblay, Phys. Rev. B **49**, 13267 (1994)
60. A.-M.S. Tremblay, B. Kyung, D. Sénéchal, Fiz. Nizk. Temp. (Low Temp. Phys., Ukraine) **32**, 561 (2006)
61. B. Davoudi, A.-M.S. Tremblay, Phys. Rev. B **76**, 085115 (2007)
62. N.E. Bickers, D.J. Scalapino, S.R. White, Phys. Rev. Lett. **62**, 961 (1989)
63. P. Monthoux, D.J. Scalapino, Phys. Rev. Lett. **72**, 1874 (1994)
64. D. Manske, I. Eremin, K.H. Bennemann, in *The Physics of Conventional and Unconvencional Superconductors*, edited by K.H. Bennemann, J.B. Ketterson (Springer-Verlag, Berlin, 2004), Vol. II, p. 731
65. R. Shankar, Rev. Mod. Phys. **66**, 129 (1994)
66. W. Metzner, C. Castellani, C. Di Castro, Adv. Phys. **47**, 317 (1998)
67. S.A. Kivelson, E. Fradkin, V. Oganesyan, I.P. Bindloss, J.M. Tranquada, A. Kapitulnik, C. Howald, Rev. Mod. Phys. **75**, 1201 (2003)
68. M. Vojta, Adv. Phys. **58**, 699 (2009)
69. N. Furukawa, T.M. Rice, M. Salmhofer, Phys. Rev. Lett. **81**, 3195 (1998)
70. C. Honerkamp, M. Salmhofer, N. Furukawa, T.M. Rice, Phys. Rev. B **63**, 035109 (2001)
71. C. Honerkamp, H.C. Fu, D.-H. Lee, Phys. Rev. B **75**, 014503 (2007)
72. C.J. Halboth, W. Metzner, Phys. Rev. B **61**, 7364 (2000)
73. C.J. Halboth, W. Metzner, Phys. Rev. Lett. **85**, 5162 (2000)
74. E. Dagotto, Rev. Mod. Phys. **66**, 763 (1994)
75. N. Bulut, Adv. Phys. **51**, 1587 (2002)
76. D.J. Scalapino, in *Handbook of High-Temperature Superconductivity. Theory and Experiment*, edited by J.R. Schrieffer, J.S. Brooks (Springer-Verlag, New York, 2007), pp. 495–526
77. Th. Maier, M. Jarrel, Th. Pruschke, M.H. Hettler, Rev. Mod. Phys. **77**, 1027 (2005)
78. Th.A. Maier, M. Jarrell, D.J. Scalapino, Phys. Rev. Lett. **96**, 047005 (2006)
79. Th.A. Maier, M. Jarrell, D.J. Scalapino, Phys. Rev. B **74**, 094513 (2006)
80. S.S. Kancharla, B. Kyung, D. Sénéchal, M. Civelli, M. Capone, G. Kotliar, A.-M.S. Tremblay, Phys. Rev. B **77**, 184516 (2008)
81. A. Avella, F. Mancini, Phys. Rev. B **75**, 134518 (2007)
82. A. Avella, F. Mancini, J. Phys.: Condens. Matter **19**, 255209 (2007)
83. A. Macridin, M. Jarrell, Phys. Rev. B **79**, 104517 (2009)
84. T. Aimi, M. Imada, J. Phys. Soc. Jpn **76**, 13708 (2007)
85. R.O. Zaitsev, V.A. Ivanov, Soviet Phys. Solid State **29**, 2554 (1987)
86. R.O. Zaitsev, V.A. Ivanov, Soviet Phys. Solid State **29**, 3111 (1987)
87. R.O. Zaitsev, V.A. Ivanov, Int. J. Mod. Phys. B **5**, 153 (1988)
88. N.M. Plakida, V.Yu. Yushankhai, I.V. Stasyuk, Physica C **160**, 80 (1989)
89. V.Yu. Yushankhai, N.M. Plakida, P. Kalinay, Physica C **174**, 401 (1991)
90. N.M. Plakida, V.S. Oudovenko, Phys. Rev. B **59**, 11949 (1999)
91. P. Prelovšek, A. Ramšak, Phys. Rev. B **72**, 012510 (2005)
92. V.V. Val'kov, T.A. Val'kova, D.M. Dzebisashvili, S.G. Ovchinnikov, JETP Lett. **75**, 378 (2002)
93. J. Jędrak, J. Spałek, Phys. Rev. B **81**, 073108 (2010)
94. J. Jędrak, J. Spałek, Phys. Rev. B **83**, 104512 (2011)
95. J. Beenen, D.M. Edwards, Phys. Rev. B, **52**, 13636 (1995)
96. A. Avella, F. Mancini, D. Villani, H. Matsumoto, Physica C **282–287**, 1757 (1997)
97. T. Di Matteo, F. Mancini, H. Matsumoto, V.S. Oudovenko, Physica B **230–232**, 915 (1997)
98. T.D. Stanescu, I. Martin, Ph. Phillips, Phys. Rev. B **62**, 4300 (2000)
99. N.M. Plakida, R. Hayn, Z. Phys. B **93**, 313 (1994)
100. E.I. Shneider, S.G. Ovchinnikov, Zh. Eksp. Teor. Fiz. **136**, 1177 (2009)
101. R. Khasanov, A. Shengelaya, E. Morenzoni, K. Conder, I.M. Savić, H. Keller, J. Phys.: Condens. Matter **16**, S4439 (2004)
102. N.M. Plakida, Phys. Scr. **83**, 038303 (2011)
103. P.W. Anderson, Adv. Phys. **46**, 3 (1997)
104. E. Plekhanov, S. Sorella, M. Fabrizio, Phys. Rev. Lett. **90**, 187004 (2003)
105. S. Raghu, R. Thomale, T.H. Geballe, Phys. Rev. B **86**, 094506 (2012)
106. D. Sénéchal, A. Day, V. Bouliane, A.-M.S. Tremblay, `arXiv:1212.4503` (unpublished)